Infrared Spectra of Molecules and Materials of Astrophysical Interest

Grant NGL-41-002-003
Quarterly Progress Report
Report Number 36
June 1976

Office of Grants and Research Contracts
Office of Space Science and Applications
National Aeronautics and Space Administration
Washington, D. C. 20546

(Prepared under Grant NGL-41-002-003 by the

University of South Carolina, Columbia, South Carolina 29208

Principal Investigator: James R. Durig, Professor of Chemistry

Period Covered: 15 March 1976 to 15 June 1976

SUMMARY OF PROGRESS

We have been studying the vibrational spectra from 4000 to 33 cm^{-1} of several molecules which may be present in the atmosphere of the Jovian planets or exist in outer space. These studies have been made to provide vibrational frequencies which can be used to: (1) determine the composition of the cloud covers of several of the planets, (2) provide structural information under favorable circumstances, (3) provide necessary data from which accurate thermodynamic data can be calculated, and (4) furnish information as to the nature of the potential energy function of the molecules and forces acting within them.

Some of the molecules which we have studied can be produced photochemically from methane, ammonia, and hydrogen sulfide which are thought to be constituents of the planets with reducing atmospheres. Some of the compounds will polymerize under ultraviolet radiation and drop out of the atmospheres. However, planets with a hot base, like that of Jupiter, may rebuild molecules destroyed photochemically. Therefore, we have used these criteria in selecting the compounds which we have studied.

Gerald P. Kuiper[1] has pointed out that the Jovian atmosphere is expected to contain H_2, He, N_2, H_2O, NH_3, CH_3, Ar and possibly SiH_4. He has also listed a number of other gases that should be considered because they are composed of fairly abundant atomic species and have boiling points below 120°C (see Table 8, pg. 349-350 of reference 1). He has also pointed out that until more is known about the atmospheres of the planets, it is useful to keep a fairly large number of possible constituents in mind in planning further spectroscopic work.

In our initial work on the vibrational spectra of molecules of astrophysical interest, we studied hydrazine,[2] methylamine,[3] as well as several substituted hydrazines.[4-8] Recently both ethane and acetylene have been found in the atmosphere of Jupiter.[9] It is expected that substituted ethanes will also be eventually found in some of the planetary atmospheres. In fact, ethanol has been found in the Sagittarius B12 cloud of dust and gas which is near the center of the Milky Way.[10] In addition, molecules such as acetaldehyde (CH_3CHO), methanol (CH_3OH), dimethylether $(CH_3)_2O$, formic acid (HCOOH), have been identified in outer space. As a continuation of our earlier studies on the low frequency torsional motions of dimethylether[11] we have recorded the high resolution microwave spectra of this molecule along with the two isotopic derivatives, CH_3OCD_3 and $(CD_3)_2O$ and reported this study in the last progress report. We have now completed the relatively high resolution far infrared study along with a study of the low frequency Raman spectra of the gas.

Several years ago the gas phase far infrared spectra of molecules of the type $(CH_3)_2X$ and $(CD_3)_2X$ were published. Some of these spectra showed a very complex pattern in the region where the methyl torsional transitions are expected. Tuazon and Fateley[12] reported in 1971 the far infrared spectrum of CD_3OCH_3 along with the already measured species $(CH_3)_2O$ and $(CD_3)_2O$. The spectrum of this compound is similarly complex. These authors took the most likely band in the spectra to obtain an estimate of the barrier height, but detailed interpretation of the complex features were not presented. To our knowledge, only one Raman spectrum of gaseous CH_3OCH_3 has been reported. In 1957, Taylor and Vidale[13] reported two Raman bands at 480 and 450 cm^{-1} as overtones of both torsional modes.

In order to get better barrier information on these isotopic species of dimethylether and eventually to explain the complicated structure of their

far infrared spectra, the Raman spectra of these isotopes were measured in the gas phase on a Cary Model 82 instrument with a Spectra Physics 171 argon ion laser. For the same purpose, the far infrared spectra were remeasured with 0.5 cm^{-1} resolution with a Digilab FTS 15B interferometer. In Figure 1 are shown the far infrared spectrum of the normal isotope. The band at 240 cm^{-1} is clearly asymmetric, and the band at 223 cm^{-1} is split into at least three components at 223.2, 224.8 and 226.0 cm^{-1}. Minor bands occur around 200 cm^{-1}. The 240 cm^{-1} band has been interpreted previously as the $0 \rightarrow 1$ transition of the infrared active torsion. But the 223 cm^{-1} band is not the $1 \rightarrow 2$ transition of the same mode, as one might believe. If this were the case, the overtone band should occur at 463 cm^{-1}. The Raman spectrum in Figure 2 clearly shows that there is no band at this frequency. There are bands at 480 and 450 cm^{-1}, as previously reported, in addition to the bending mode at 412 cm^{-1}. Knowing the far infrared spectrum, the 480 cm^{-1} band may really be interpreted as the overtone of the infrared active torsion, assuming that the 240 cm^{-1} band consists of at least two torsional transitions. The infrared inactive mode was estimated by Fateley and Miller[14] and several normal coordinate calculations to be at about 200 cm^{-1}. Therefore, the 395 cm^{-1} band could well be the overtone of this torsion. All Raman bands are strongly polarized. In the torsional region, only a very broad, very weak Raman signal with no structure was observed.

In order to check this preliminary assignment and to determine a better potential function, a computer program has been developed. It solves the eigenvalue problem of the internal Hamiltonian of any model with two internal rotors of C_{3v} symmetry (see Table I). Since the models for dimethylether d_0, d_3 and d_6 have higher symmetry than the most general model, some of the terms in this operator vanish or have equal coefficients. The program is set up in the direct product basis of two exponential basis sets and uses a diagonalization subroutine for complex Hermitian matrices. It first solves the eigenvalue

problems of the single top models (first and second line, respectively) and transforms the matrices of the operators $\hat{P}_i$, cos $3\tau_i$ and sin $3\tau_i$ into their eigenbasis. Using direct product calculus, the Hamiltonian matrix is set up for the coupled problem and diagonalized. A standard iteration routine allows the fitting of observed transition frequencies and determination of the potential coefficients. It further calculates the squares of the matrix elements of cos $3\tau_i$ and sin $3\tau_i$ and weights them with the Boltzman population factor. These numbers are used to identify the energy levels with respect to the symmetry of the two top model and to obtain rough estimates of relative intensities of the transitions. With this program, the fit in Table II was obtained. It looks quite reasonable. However, it does not explain the weak Raman band at 363 cm^{-1}. Another weak Raman band at 381 cm^{-1} may eventually be interpreted as a line belonging to a different torsional substate of the 385 cm^{-1} band, although the calculated splitting is not larger than 2 cm^{-1}. Another point which is not quite satisfactory is the fact that the intensity ratio of the 450 and 480 cm^{-1} bands is about 1:2, the calculated ratio, however, is about 1:10. For the present, this fit seems to be the best we can find and the corresponding potential coefficients are given in the lower half of Table II. For comparison, the results of a recent microwave investigation of ground state and two torsionally excited states splittings are given. Instead of using $V_{30} = V_{03}$, V_{33} and V'_{33} to define the potential function, an identical function may be written as

$$2V = V_{30}(1-c3\tau_0)(1-c3\tau_1) + V_{eff}(1-c3\tau_0c3\tau_1) + V'_{33}s3\tau_0s3\tau_1.$$

The coefficients in this equation have lower dispersions and are much less correlated to each other. They are also given in Table II.

In Figure 3 is shown the far infrared spectrum of CD_3OCH_3. Due to the higher resolution, it shows a lot more features than the previously published spectrum. Note the band series at 162.0, 154.5, 145.2 and 133.2 cm^{-1}. They

may be assigned to the $0 \rightarrow 1$, $1 \rightarrow 2$, $2 \rightarrow 3$ and $3 \rightarrow 4$ transitions of the CD_3 torsional mode. In the region of the "light" methyl torsion, the interpretation is not straightforward. The main features are at 224.0, 222.0, 218.2, 210.7 and 204.9 cm^{-1}, all but the first two are rather broad and probably consisting of more than one torsional transition. The Raman spectrum, shown in Figure 4 is similarly complex in the overtone region. The bending mode at 373 cm^{-1} is relatively weak compared with the light isotope. Bands of similar intensities appear at 384 and 380 cm^{-1}, the former being assigned to the lowest combination transition of both torsions. The weak band at 316.5 cm^{-1} is assigned as the $0 \rightarrow 2$ transition of the CD_3 torsion, since its frequency is the sum of 162.0 and 154.5 cm^{-1} which corresponds to two infrared transitions. The 442 cm^{-1} band is the sum of 224 and 218 cm^{-1}; therefore, this band is assigned to the $0 \rightarrow 2$ transition of the light methyl torsion. We suspect Fermi resonance type interactions to be responsible for the particular intensity pattern in the 380 cm^{-1} region, although a good frequency fit could be obtained without this assumption. The results of the fit are represented in Table III. This fit again is reasonable, although it does not explain everything, for instance, the infrared absorption at 210 cm^{-1}. Again, the potential function can be expressed by different coefficients. One choice is to use V_s, V_d and V_{seff} in the form

$$2V = V_s(1-c3\tau_0)(1-c3\tau_1) + V_d(\cos 3\tau_2 - c3\tau_1) + V_{seff}(1-c3\tau_0 c3\tau_1) + V'_{33}s3\tau_0 s3\tau_1.$$

The coefficients are also given in this Table III, the correlations are weaker than in the original set and they are better determined.

The Raman spectrum of CD_3OCD_3 in Figure 5 shows, besides the bending mode, at least 15 different polarized lines. At present, no interpretation can be given since the analysis has not been completed yet.

The agreement between the potential coefficients of different isotopes is not very exciting. Similarly, there are certain discrepancies with the results of the microwave splittings analysis. Several reasons may be responsible for

these facts. The present assignment may not be correct since, as already pointed out, several features of the spectra can not be explained, although we tried quite a number of possiblities. The microwave analysis was performed using splittings in the ground state and two excited states. We think that from this information, at most, three and probably only two potential coefficients can be determined. The torsional analysis, however, includes transitions involving energy levels almost to the top of the effective barrier, so that the information about the higher parts of the potential surface should be much better than in the microwave investigation. Despite these doubts, the cos-cos coupling term is definitely a large number and it has definitely no relation at all with the sin-sin coefficient which has been proposed in some earlier work.

Table I

Hamiltonian and Basis Functions

$$\hat{H} = \tfrac{1}{2}g^{44}\hat{p}_0^{\,2} + \tfrac{1}{2}\{V_{30}(1-\cos 3\tau_0) + V_{60}(1-\cos 6\tau_0) + V'_{60}\sin 6\tau_0\}$$
$$+ \tfrac{1}{2}g^{55}\hat{p}_1^{\,2} + \tfrac{1}{2}\{V_{03}(1-\cos 3\tau_1) + V_{06}(1-\cos 6\tau_1) + V'_{06}\sin 6\tau_1\}$$
$$+ g^{45}\hat{p}_0\hat{p}_1 + \tfrac{1}{2}\{V_{33}(\cos 3\tau_0\cos 3\tau_1 - 1) + V'_{33}\sin 3\tau_0\sin 3\tau_1$$
$$+ V''_{33}\sin 3\tau_0\cos 3\tau_1 + V'''_{33}\cos 3\tau_0\sin 3\tau_1\}$$

$$\{\Phi_{mn}(\tau_0,\tau_1)\} = \{\phi_m(\tau_0)\} \times \{\phi_n(\tau_1)\}$$

$$\phi_\ell(\tau_j) = (2\pi)^{-\frac{1}{2}} \exp(i\ell\tau_j)$$

CH_3OCH_3, CD_3OCD_3: $g^{44} = g^{55}$; $V_{30} = V_{03}$; $V_{60} = V_{06}$; $V'_{60} = V'_{06} = V''_{33} = V'''_{33} = 0$

CD_3OCH_3: $V'_{60} = V'_{06} = V''_{33} = V'''_{33} = 0$

Table II

Fit of Torsional Frequencies for CH_3OCH_3

$g^{44} = g^{55} = 13.5644\ cm^{-1}$ $\quad g^{45} = -2.7381\ cm^{-1}$

Transition	Obs(cm^{-1})	Calc(cm^{-1})	Obs-Calc	Transition	Obs(cm^{-1})	Calc(cm^{-1})	Obs-Calc
1→3	241.0	243.8	-2.8	1→6	481.3	484.2	-2.9
3→6	239.9	240.4	-0.5	2→9	450.2	446.9	3.3
2→5	223.2	222.7	0.5	1→4	395.5	397.3	-1.8
5→9	226.0	224.2	1.8	2→7	385.2	383.8	1.4
4→8	200.7	199.7	1.0				
5→9	224.8	223.4	1.4	} These transitions were not fitted. They are assigned			
4→8	199.0	198.1	0.9	} to different torsional substates.			

Standard deviation of frequencies 2.51 cm^{-1}

Potential Coefficients (cm^{-1})[a]		Microwave	Derived Potential Coefficients		Microwave[b]
$V_{30}=V_{03}$	1132.91±37.52	909.05±0.25	$V_{eff} = V_{30}-V_{33}$	918.66±10.95	909.05±0.25
V_{33}	214.25±47.09	0(not varied)			
V'_{33}	20.92 ± 8.05	10.12±1.60			
$V_{60}=V_{06}$	0(not varied)	0(not varied)			

[a] Error limit = dispersion of parameter

[b] J. R. Durig, Y. S. Li and P. Groner, accepted for publication (J. Mol. Spectry).

Table III

Fit of Torsional Frequencies for CD_3OCH_3

g^{44} = 13.0973 cm^{-1} g^{55} = 8.1872 cm^{-1} g^{45} = -2.4764 cm^{-1}

Transition	Obs(cm^{-1})	Calc(cm^{-1})	Obs-Calc	Transition	Obs(cm^{-1})	Calc(cm^{-1})	Obs-Calc
1→2	162.0	161.8	0.2	1→3	224.0	225.9	-1.9
2→4	154.5	155.3	-0.8	3→6	218.2	218.3	-0.1
4→7	145.2	145.6	-0.4	1→6	442.0	444.2	-2.2
7→10	133.0	131.8	1.2	3→11	435.0	433.6	1.4
1→4	316.5	317.2	-0.7	2→5	222.0	221.9	0.1
1→5	384.0	383.7	0.3	5→9	204.9	202.2	2.7
2→8	380.0	381.1	-1.1	6→11*	215.8 sh	215.3	0.5
3→9	361.5	360.0	1.5	* not fitted			

Standard deviation of frequencies 1.55 cm^{-1}

Potential Coefficients (cm^{-1})[a]		Microwave[b]	Derived Potential Coefficients		Microwave[b]
V_{30}	1313.52±30.31	910.45±0.17	$V_s = \frac{1}{2}(V_{30}+V_{03})$	1285.97±30.08	903.81±0.65
V_{03}	1258.41±30.45	897.18±1.21	$V_d = \frac{1}{2}(V_{30}-V_{03})$	27.55 ± 4.24	6.64±0.56
V_{33}	417.11±35.54	0(not varied)	$V_{seff} = V_s - V_{33}$	868.85 ± 6.14	903.81±0.65
V'_{33}	34.22 ± 7.99	0(not varied)	$V_{30eff} = V_{30} - V_{33}$	896.41 ± 6.99	910.45±0.17
$V_{06}=V_{60}$	0(not varied)	0(not varied)	$V_{03eff} = V_{03} - V_{33}$	841.30 ± 7.92	897.18±1.21

[a] Error limit = dispersion of parameter

[b] J. R. Durig, Y. S. Li and P. Groner, accepted for publication (J. Mol. Spectry).

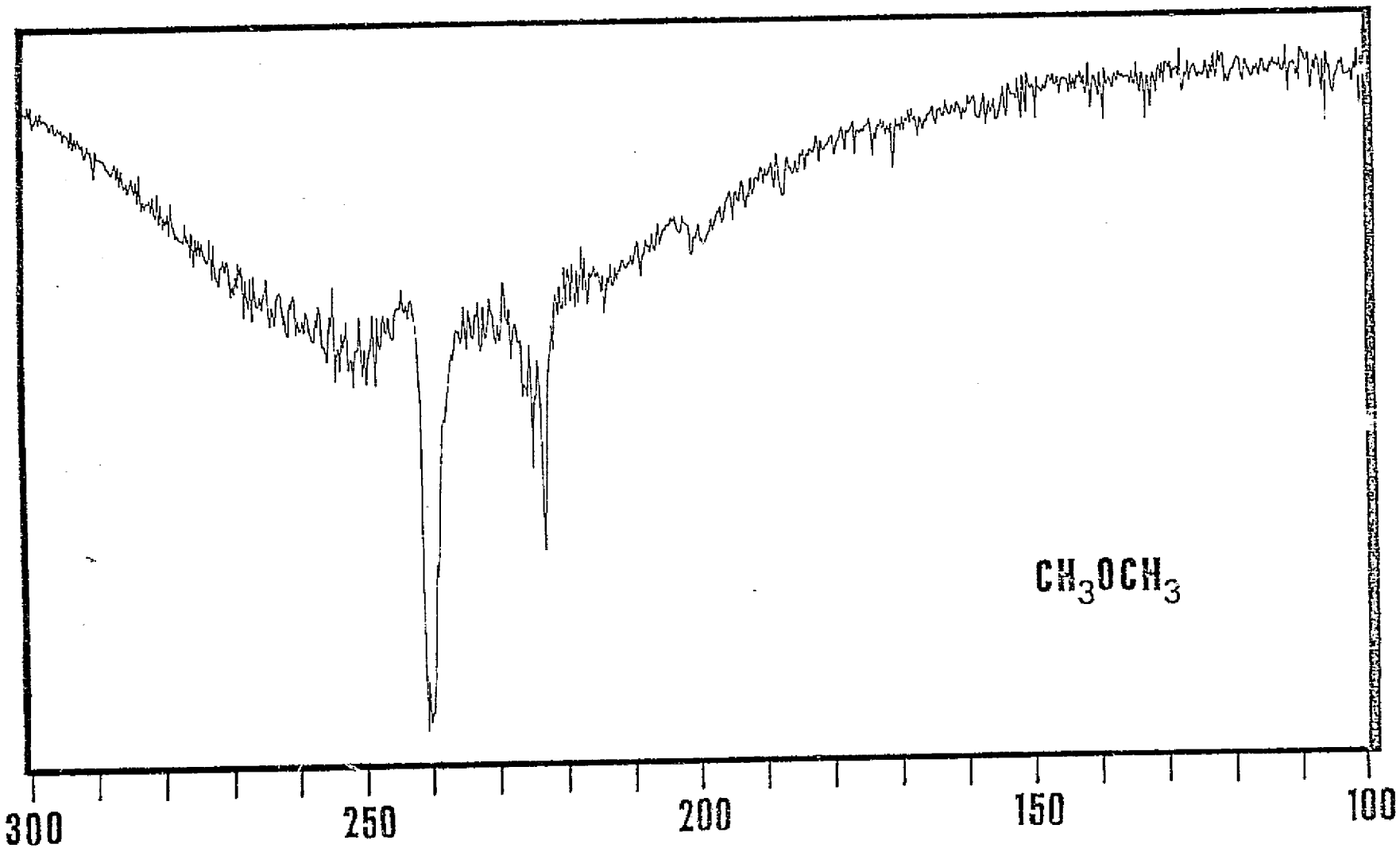
CH_3OCH_3
300
250
200
150
100

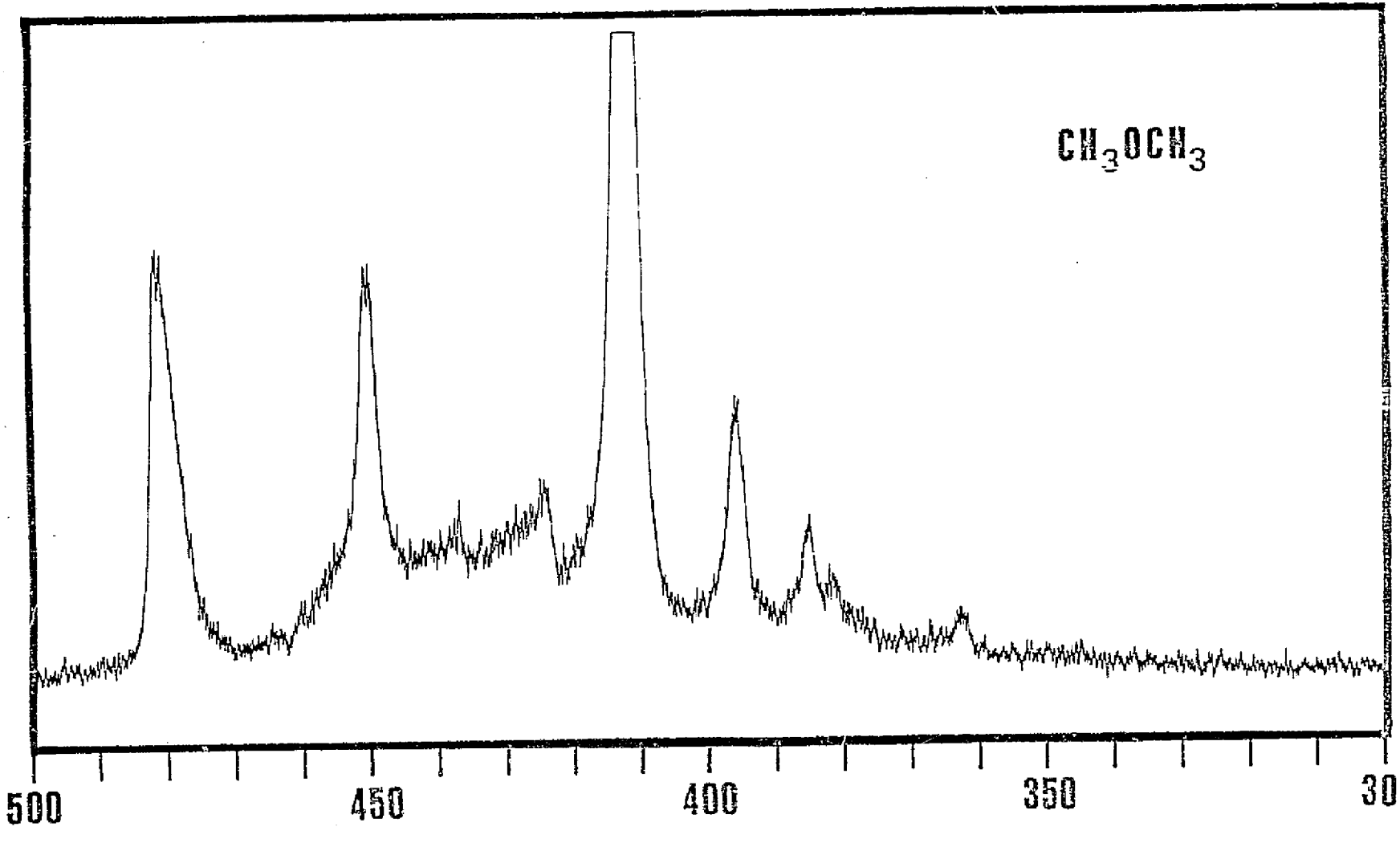
CH_3OCH_3
500
450
400
350
300

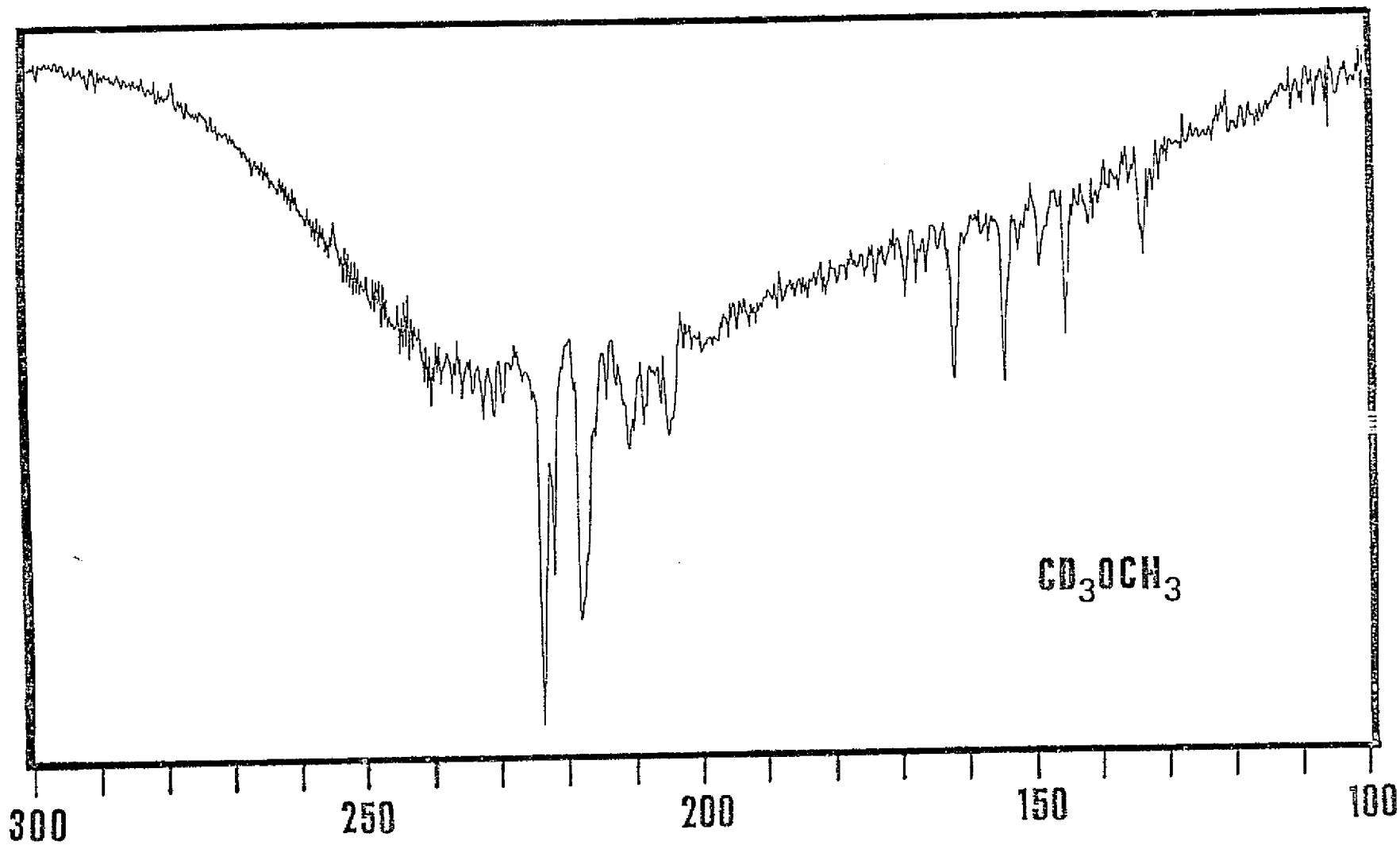
CD_3OCH_3
300
250
200
150
100

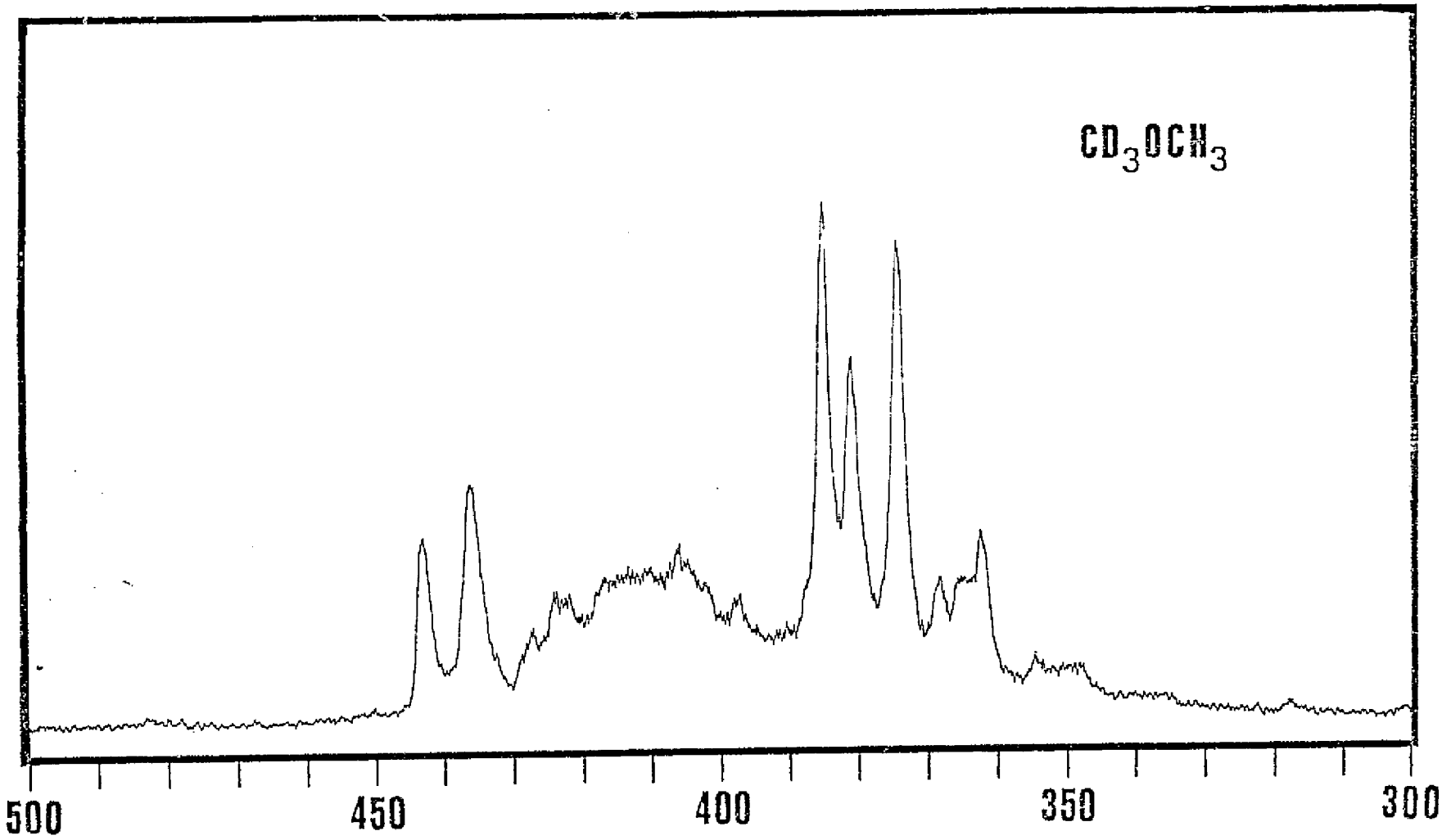
CD_3OCH_3
500
450
400
350
300

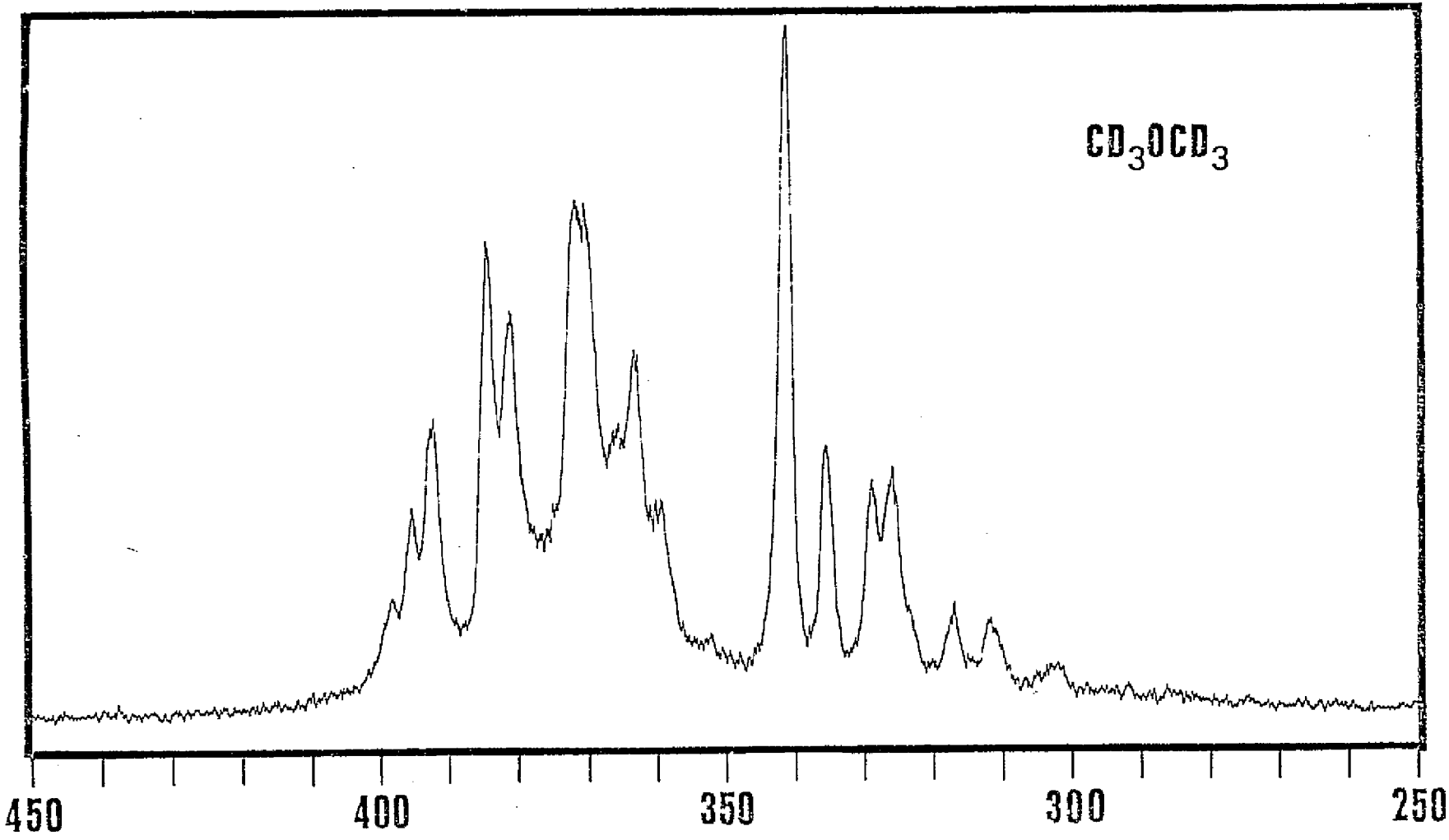
CD_3OCD_3
450
400
350
300
250

Although this study is not yet complete, we should be able to provide a complete manuscript by the next progress report time.

For several progress reports we have mentioned our work on methylchloroformate and anticipated that this work would soon be finished. We are pleased to report that a manuscript has been submitted to the Journal of Molecular Spectroscopy on this molecule.

The structure of methylchloroformate has been the subject of considerable interest. Four dipole moment studies have been reported.[15-18] From two of these[15,17] the results were interpreted in terms of a planar s-cis structure. The data from the other dipole moment studies[16,18] were interpreted in terms of a planar s-trans structure.

Three analyses of the vibrational spectra have been reported.[19-21] These analyses were all in terms of a molecular model of C_s symmetry and were consistent with an s-trans structure. An electron diffraction study of the vapor of methylchloroformate was performed.[22] The data yielded only an s-trans structure that was slightly non-planar with the methyl group approximately 20° out of the plane of the other heavy atoms.

An investigation of the infrared spectrum and of the proton NMR spectrum of methylchloroformate in solution was reported.[23] The authors found evidence for the coexistence of both the s-cis and the s-trans conformations and indicated that the s-cis was more stable. From a study comparing observed and calculated ^{35}Cl nuclear quadrupole resonance frequencies the authors[24] concluded that the s-trans was the most likely stable structure in the solid.

A microwave spectroscopic investigation[25] of natural abundance ^{35}Cl and ^{37}Cl isotopic species of methylchloroformate showed that the planar s-trans molecular structure was most consistent with the data. Small amounts of a second rotamer, however, could not be precluded.

Therefore, in an effort to clear up the ambiguities in the conformational preferences of methylchloroformate and to provide more complete structural data, the investigation of the microwave, Raman and far infrared spectra of the vapor were undertaken. The results of this study can be summarized by the abstract which follows of the paper that has been submitted for publication.

Abstract: The microwave spectra of six isotopic species of methylchloroformate, $ClCO_2CH_3$, have been recorded from 18.0 to 40.0 GHz. Structural parameters have been determined and it is shown that the only stable conformer at ambient temperature is the s-trans. From the Stark effect, the dipole moment components were determined to be $|\mu_a| = 1.7 \pm 0.2$, $|\mu_b| = 1.0 \pm 0.2$, and $|\mu_t| = 2.0 \pm 0.2$D. The Raman and far infrared spectra of the vapor are reported. Four cases of Fermi resonance have been observed in the Raman effect. Both the methyl and methoxy torsions have been observed in the far infrared and the methyl barrier to internal rotation has been determined to be 1.15 kcal/mole (1.19 kcal/mole for the CD_3 rotor) which is lower than the 1.23 kcal/mole obtained from the microwave splitting method. It is shown from both the ^{13}C and ^{1}H NMR spectra that only one conformer exists which is contrary to what was previously reported. The vibrational spectrum of the solid is also reported and discussed.

For the complete paper, see appendix I of this report.

In addition to our studies of carbonyl containing compounds, we have been pursuing investigations on the vibrational and rotational spectra of a number of nitrogen and phosphorus containing compounds which are likely to be found in the atmospheres of the Jovian planets. In earlier progress reports we reported the vibrational spectra and structure of dimethylphosphine, ethylphosphine and isopropylphosphine. As a continuation of these studies, we have investigated the vibrational spectrum of tertiary-butylphosphine.

Vibrational spectroscopy has been shown to be a valuable tool in the determination of intramolecular potential functions governing internal rotation about single bonds.[26,27] This method has recently been extended to the study of asymmetric tops rotating against a molecular frame, as opposed to the more familiar symmetric tops such as $-CH_3$ and $-SiH_3$.[28] If the molecular frame is asymmetric as well, it is possible for there to be spectroscopically distinct rotational isomers or conformers. Both ethylphosphine ($CH_3CH_2PH_2$) and isopropylphosphine [$(CH_3)_2CHPH_2$] are examples of this type of system since the PH_2 group constitutes an asymmetric internal rotor. The internal rotation barrier for the PH_2 top has been determined for both of these molecules.[29,30] If, however, the molecular frame is symmetric, as is the case in tertiary-butylphosphine, [$(CH_3)_3CPH_2$], only one conformation is possible and the potential function governing internal rotation is considerably simplified, becoming three-fold symmetric as in the case of methylphosphine (CH_3PH_2). Thus, the determination of this potential function for t-butylphosphine is a natural extension of the prior studies of ethyl-[29] and isopropylphosphine.[30] Also, it would be of interest to determine the barriers to internal rotation of the methyl groups in this molecule, as part of continuing studies[31,32] of the top-top interactions in such "three-top" molecules.

Finally, the assignment of the vibrational spectrum of t-butylphosphine would finish the series of singly alkyl-substituted phosphines: methyl, ethyl

and isopropyl. Group frequencies determined for the PH_2 moiety from these studies could be expected to apply to almost any hydrocarbon derivative. The results of this study have been submitted for publication in the Journal of Molecular Structure and can be summarized by the abstract of the paper (see appendix II for the complete paper).

ABSTRACT: The infrared spectra of gaseous and solid tertiary-butylphosphine, $[(CH_3)_3CPH_2]$, have been recorded from 50 cm^{-1} to 3500 cm^{-1}. The Raman spectra of gaseous, liquid and solid $(CH_3)_3CPH_2$ have been recorded from 10 to 3500 cm^{-1}. A vibrational assignment of the 42 normal modes has been made. A harmonic approximation of the methyl torsional barrier from observed transitions in the solid state gave a result of 4.22 kcal/mole and 3.81 kcal/mole in the gaseous state. Hot band transitions for the phosphino torsional mode have been observed. The potential function for internal rotation about the C-P bond has been calculated. The two potential constants were determined to be:

V_3 = 2.79±0.01 kcal/mole and V_6 = 0.07±0.01 kcal/mole.

FUTURE WORK

Studies are nearly complete on $(CH_3)_2NH$ and the closely related silane, $(CH_3)_2NSiH_3$. The papers are currently being written on both of these compounds. For the dimethylamine work we have written a new computer program for the interpretation of the torsional data for the two-top case. We have also undertaken a study of the vibrational spectrum of isopropyl amine. Studies have also been initiated on the low frequency spectra of dimethylphosphine. Vibrational work is also being done on propylaldehyde. We shall also continue our current work on several compounds which have potential interest as planetary atmosphere materials.

References

1. G. P. Kuiper, Atmospheres of the Earth and Planets, University of Chicago Press, Chicago, 1952.

2. J. R. Durig, S. F. Bush, and E. E. Mercer, J. Chem. Phys., 44, 4238 (1966).

3. J. R. Durig, S. F. Bush, and F. G. Baglin, J. Chem. Phys., 49, 2106 (1968).

4. J. R. Durig, W. C. Harris, and D. W. Wertz, J. Chem. Phys., 50, 1449 (1969).

5. J. R. Durig and W. C. Harris, J. Chem. Phys., 51, 4457 (1969).

6. J. R. Durig and W. C. Harris, J. Chem. Phys., 55, 1735 (1971).

7. J. R. Durig, R. W. MacNamee, L. B. Knight, and W. C. Harris, Inorg. Chem., 12, 804 (1973).

8. J. R. Durig, J. W. Thompson, and J. D. Witt, Inorg. Chem., 11, 2477 (1972).

9. Chen. Eng. News, 4, 4 (1974).

10. Ind. Res., May 1974, page 29, by Nat. Radio Astronomy Observatory at Kitt Peak.

11. J. R. Durig, C. M. Player, Jr., J. Bragin and Y. S. Li, J. Chem. Phys., 55, 2895 (1971).

12. E. C. Tuazon and W. G. Fateley, J. Chem. Phys., 54, 4450 (1971).

13. R. C. Taylor and G. L. Vidale, J. Chem. Phys., 26, 122 (1957).

14. W. G. Fateley and F. A. Miller, Spectrochim. Acta, 18, 977 (1962).

15. S. Mizushima and M. Kubo, Bull. Chem. Soc. Jap., 13, 174 (1938).

16. R. J. W. LeFevre and A. Sundaram, J. Chem. Soc. (Lond.) 1962, 3904.

17. E. Bock and D. Iwacha, Can. J. Chem., 45, 3177 (1967).

18. M. J. Aroney, R. J. W. LeFevre, R. K. Pierens, and H. L. K. The, Aust. J. Chem., 22, 1599 (1969).

19. B. Collingwood, H. Lee, and J. K. Wilmshurst, Aust. J. Chem., 19, 1637 (1966).

20. R. A. Nyquist, Spectrochim. Acta, 28A, 285 (1972).

21. J. E. Katon and M. G. Griffin, J. Chem. Phys., 59, 5868 (1973).

22. J. M. O'Gormm, W. Shand, Jr., and V. Schomaker, J. Amer. Chem. Soc., 72, 4222 (1950).

23. M. Oki and H. Nakanishi, Bull. Chem. Soc. Jap., 45, 1552 (1972).

24. A. J. Cohen and M. A. Whitehead, J. C. S. Faraday II, 68, 649 (1972).

25. D. G. Lister and N. L. Owen, J. C. S. Faraday II, 69, 1036 (1973).

26. J. R. Durig, S. M. Craven, and W. C. Harris, Vibrational Spectra and Structure, Vol. 1, J. R. Durig, ed., Marcel Dekker, New York, N.Y., 73-179 (1972).

27. A. V. Cunliffe, Internal Rotation in Molecules, W. J. Orville-Thomas, ed., John Wiley and Sons, New York, N.Y., 217-252 (1974).

28. W. G. Fateley, Pure App. Chem., 36, 119 (1973).

29. J. R. Durig and A. W. Cox, Jr., J. Chem. Phys., 63, 2303 (1975)

30. J. R. Durig and A. W. Cox, Jr., J. Phys. Chem., 80, 000 (1976).

31. J. R. Durig, S. M. Craven and J. Bragin, J. Chem. Phys., 51, 5663 (1969).

32. J. R. Durig, S. M. Craven, J. H. Mulligan and C. W. Hawley, J. Chem. Phys., 58, 1281 (1973).

APPENDIX I

THE MICROWAVE, RAMAN, FAR INFRARED AND NMR SPECTRA, STRUCTURE AND DIPOLE MOMENT OF METHYLCHLOROFORMATE

Abstract

The microwave spectra of six isotopic species of methylchloroformate, $ClCO_2CH_3$, have been recorded from 18.0 to 40.0 GHz. Structural parameters have been determined and it is shown that the only stable conformer at ambient temperature is the s-trans. From the Stark effect the dipole moment components were determined to be $|\mu_a| = 1.7 \pm 0.2$, $|\mu_b| = 1.0 \pm 0.2$, and $|\mu_t| = 2.0 \pm 0.2$D. The Raman and far infrared spectra of the vapor are reported. Four cases of Fermi resonance have been observed in the Raman effect. Both the methyl and methoxy torsions have been observed in the far infrared and the methyl barrier to internal rotation has been determined to be 1.15 kcal/mole (1.19 kcal/mole for the CD_3 rotor) which is lower than the 1.23 kcal/mole obtained from the microwave splitting method. It is shown from both the ^{13}C and ^{1}H NMR spectra that only one conformer exists which is contrary to what was previously reported. The vibrational spectrum of the solid is also reported and discussed.

INTRODUCTION

The structure of methylchloroformate has been the subject of considerable interest. Four dipole moment studies have been reported.[1-4] From two of these[1,3] the results were interpreted in terms of a planar s-cis strucutre. The data from the other dipole moment studies[2,4] were interpreted in terms of a planar s-trans structure (Fig. 1).

Three analyses of the vibrational spectra have been reported.[5-7] These analyses were all in terms of a molecular model of C_s symmetry and were consistent with an s-trans structure. An electron diffraction study of the vapor of methylchloroformate was performed.[8] The data yielded only an s-trans structure that was slightly non-planar with the methyl group approximately 20° out of the plane of the other heavy atoms.

An investigation of the infrared spectrum and of the proton NMR spectrum of methylchloroformate in solution was reported.[9] The authors found evidence for the coexistence of both the s-cis and the s-trans conformations and indicated that the s-cis was more stable. From a study comparing observed ard calculated ^{35}Cl nuclear quadrupole resonance frequencies the authors[10] concluded that the s-trans was the most likely stable structure in the solid.

A microwave spectroscopic investigation[11] of natural abundance ^{35}Cl and ^{37}Cl isotopic species of methylchloroformate showed that the planar s-trans molecular strucutre was most consistent with the data. Small amounts of a second rotamer, however, could not be precluded.

Therefore, in an effort to clear up the ambiguities in the conformational preferences of methylchloroformate and to provide more complete structural data, the investigation of the microwave, Raman and far infrared spectra of the vapor were undertaken.

EXPERIMENTAL

Practical grade methylchloroformate was purchased from Aldrich Chemical Company, Incorporated and was fractionally distilled before use. The isotopic derivatives were all prepared by the reaction of the appropriate isotopic form of methanol with phosgene.[12] The CD_3OD and CH_2DOH were obtained from Merck, Sharpe and Dohme, Canada Limited. The $^{13}CH_3OH$ was purchased from Stohler Isotope Chemicals, Inc. The methanols were all used without further purification (Stated purities: CD_3OD and CH_2DOH > 95%; $^{13}CH_3OH$ 60-70%). The phosgene was obtained from Matheson and was used without further purification. The 1,2-dibromo-1,1,2,2-tetrafluoroethane was purchased from Columbia Organic Chemical Co. and was fractionally distilled before use.

The microwave spectra were recorded with a Hewlett-Packard 8460A MRR spectrometer in the 12.4-40.0 GH_z region. Samples were run both with the waveguide at room temperature and with the waveguide packed in dry ice. Sample pressures were 100 microns for survey spectra and typically 4-10 microns for measurement of the quadrupole hyperfine components. In general, the frequency accuracy should be no worse than ± 0.05 MH_z.

The Raman spectra were recorded on a Cary Model 82 spectrophotometer with a Spectra Physics Model 171 argon ion laser. The 5145Å line was used for excitation of the samples. The gas was contained at its room temperature vapor pressure in a quartz cell and the laser beam was multipassed through the cell with the standard Cary accessory. Laser power for the gas sample was 5.5 W measured at the laser head. Laser power for the solid sample was 2.0 W measured at the laser head.

The cryostat used was a Spectrim Spectrometric Sample Conditioner controlled by a Lake Shore Electronics, Inc. Cryogenic Temperature Indicator/Controller. The temperature of the sample was maintained at 18.7 ± 0.1° K

and was measured with a calibrated Silicon Diode Sensor obtained from Cryogenic Technology, Inc.

The far infrared spectra of the vapor were recorded on a Digilab Model 15B Fourier Transform Interferometer with a 12.5 micron Mylar beamsplitter. The vapor was contained in a 10 cm. glass cell with polyethylene windows at its room temperature vapor pressure. Resolution was equal to 0.5 cm^{-1}.

All NMR measurements were made on a Varian XL-100-15 NMR spectrometer equipped with a 16K (1K = 1024 words) 620I computer and a 2 million word disc (VDM-36). Temperatures were measured with a thermocouple. All spectra were obtained in the pulse Fourier Transform mode.

The ^{13}C spectra were obtained using broadband noise-modulated proton decoupling with the spectrometer locked to the ^{19}F resonance of an external sample of C_6F_6. Samples for ^{13}C measurements were 50% CH_3-O-$\overset{O}{\overset{\|}{C}}$-Cl, 50% CS_2. Proton spectra were obtained with the spectrometer locked to the ^{2}H resonance of internal CD_2Cl_2. The sample used for proton measurements was approximately 5 mM in CH_3-O-C-Cl in a 50/50 mixture of CS_2 and CD_2Cl_2. Proton T_1 measurements were obtained using the Freeman-Hill[13] inversion recovery pulse sequence. Peak heights were employed to determine the T_1 values.

MICROWAVE RESULTS

Rotational Spectra

The rotational spectra of all the isotopic species of methylchloroformate were first assigned on the basis of the known spectral pattern of a prolate asymmetric ($\kappa \simeq -0.86$) rotor compared to high pressure ($\sim$100 Torr) survey spectra. Individual lines were then remeasured at a pressure (4-10 Torr) suitable for resolution of the hyperfine splittings that result from the nuclear quadrupole coupling. The quadrupole coupling constants were then fit to the observed splitting. The positions of all observed low pressure

transitions were then corrected for quadrupole shift and used to fit the rotational constants of a rigid rotor. Initial fits were made with a-type R branch transitions and were used to approximately locate the b-type R branches. The b-type R branches were then identified by their predicted quadrupole hyperfine splittings and were used to refine the final fit of the rotational constants. The frequencies from the low pressure measurements for all the isotopic species of methylchloroformate studied here are listed in Table I. The rotational constants, moments of inertia, inertial defect, and nuclear quadrupole coupling constants for these isotopic species are listed in Table II.

STRUCTURE

The coordinates of the atoms for which isotopic substitutions were made have been calculated using the Kraitchman equations[14] and are listed in Table III. For a non-planar asymmetric top only N-3 substitutions are needed to determine the structure. This is true because there are nine moment relations:

$$Ixx = \sum_i m_i(y_i^2 + z_i^2) \qquad (1)$$

$$Ixy = -Iyx = -\sum_i m_i\, x_i\, y_i \qquad (2)$$

$$\sum_i m_i x_i = 0 \qquad (3)$$

that may be solved simultaneously. The inertial defect (Table II) for all isotopic species is indicative of an essentially planar molecule with only two hydrogens symmetrically out of the plane. For that reason the z coordinate of the atoms in the plane has been taken as zero. The nine moment relations then yield six non-trivial equations of which only five are independent. To completely solve the structure we need to calculate the six in-plane coordinates of the three unsubstituted atoms. It is, therefore, possible to calculate

the complete structure assuming only one in-plane coordinate of one of the three unsubstituted atoms.

The electron diffraction study of methylchloroformate[8] placed the carbonyl bond length at 1.19Å. From microwave studies of some related structures $r_{c=o}$ values have been calculated for COH_2 as 1.20[15], for $COCl_2$ as 1.17[16], for HCO_2CH_3 as 1.20[17], for HCO_2H as 1.20[18], for NH_2COH as 1.19[19], and for HFCO as 1.18[20]. Consideration of the carbonyl bond length listed strongly suggests that $r_{c=o}$ for methylchloroformate should be between 1.18Å and 1.20Å.

In Table IV are listed the coordinates of the three unsubstituted atoms calculated from the moment relations with the x-coordinate of the carbonyl carbon chosen so that the carbonyl bond length equals 1.19Å. The coordinates listed in Table III and Table IV reproduce the observed rotational constants in Table II to within ± 0.02%. The structural parameters calculated from these coordinates are listed in Table V. The structure of methylchloroformate is depicted in Fig. 2.

NUCLEAR QUADRUPOLE COUPLING CONSTANT

The first order chlorine nuclear quadrupole coupling constants were evaluated by a least squares fit of the observed hyperfine splittings and are listed in Table II. The value of the coupling constant along the bond axis may be calculated if the angle, θ, between the carbon-chlorine bond and the A principal axis is known using the equations:

$$\chi_{xx} \cos^2 \theta + \chi_{yy} \sin^2 \theta = \chi_{aa} \qquad (4)$$

$$\chi_{xx} \sin^2 \theta + \chi_{yy} \cos^2 \theta = \chi_{bb} \qquad (5)$$

where the x axis lies strong the carbon chlorine bond and y is perpendicular to it in the plane of the molecule and $\chi_{cc} = \chi_{zz}$. This transormation yields

χ_{xx} = -73.7 MHz, χ_{yy} = 45.1 MHz, and χ_{zz} = 28.6 for the parent molecule with θ = 20°.

These coupling constants along the bond may then be interpreted to give some information about the nature of the hybridization of the carbon-chlorine bond.[21] In the earlier microwave study of methylchloroformate the authors[11] presented such a discussion and that discussion is not significantly altered by the data presented here.

BARRIER TO INTERNAL ROTATION

The barrier to internal rotation of the methyl group was computed from the observed internal rotation splittings of the a-type and b-type R branches. The same method as adopted previously[22] was used to determine the barrier. The observed internal rotation splittings are listed in Table VI with the parameters calculated from the structure listed in Table III and IV. The value for V_3 calculated here is within the error limits of the previously determined V_3[11] value and is consistent with that found for other substituted methylformates.[23]

DIPOLE MOMENT

The second order Stark effects were observed and measured for the following components: |M| = 0,3,4 of the $5_{05} \leftarrow 4_{04}$ transition. Field calibration was accomplished by measuring the M=0 component of OCS for the J = 2←1 transition.[24] The observed and calculated Stark coefficients for $^{35}Cl\ ^{12}C\ ^{16}O_2\ ^{12}CH_3$ are listed in Table VII. The microwave spectrum associated with this molecule is quite rich. The Stark components that were tracked could be followed as a function of voltage for only 2-3 MHz before being lost in other unidentified Stark component. Considerable effort was expended in an attempt to find other suitable |M| components

to track; none were found. The error limits on the dipole components are, therefore, quite high.

VIBRATIONAL RESULTS

The Raman spectra of methylchloroformate as a vapor at room temperature and as a solid at 18.7°K are shown in Fig. 3. The far infrared spectra of gaseous methylchloroformate and methylchloroformate-d_3 are presented in Fig. 4. Transitions marked with an arrow correspond to a small amount of an impurity (HCl). The vibrational data are listed in Table VIII with their assignments.

The Raman spectrum of gaseous methylchloroformate (Fig. 4A) is largely interpretable in terms of a previously reported assignment.[7] The features at 2905 and 2845 cm^{-1} correspond to transitions observed in the Raman spectrum of the liquid[7] at 2897 and 2844 cm^{-1}. They are assigned as the overtones of the antisymmetric, ν_4/ν_{14}, and the symmetric, ν_5, methyl deformations in Fermi resonance with the symmetric CH stretch, ν_2.

The carbonyl stretch, ν_2, is assigned at 1801 cm^{-1} because it is the stronger of the two Q-branches in the region; the other Q branch (1792 cm^{-1}) is ascribed to Fermi resonance of the combination of ν_8, the COC symmetric stretch, and ν_9, the carbon chlorine stretch, (970 + 823 = 1793) with ν_2 the carbonyl stretch.

The result of another Fermi resonance interaction is apparent in the pair of Q branches at 977/962 cm^{-1}. One of the Q branches may be assigned to ν_8, the COC symmetric stretch and the other Q branch is the overtone of ν_{10}, an in-plane skeletal bend (2 X 487 = 974). The last feature of the Raman spectrum of the vapor of methylchloroformate is the Q branch series starting at 487 cm^{-1}. The relative intensity of the Q branches at 487, 480, and 472 cm^{-1} indicates they are hot bands of ν_{12}, the COC in-plane bend.

The far infrared spectra of methylchloroformate-d_0 and d_3 (Fig. 4) cover the region expected for ν_{17} and ν_{18}, the methoxy and the methyl torsions, respectively. The methoxy torsion is assigned to the Q branches at 163.2 cm^{-1} for the light compound and to the doublet at 148.8/148.2 cm^{-1} for the perdeutero compound. The apparent splitting of the Q branch for the perdeutero compound remains unexplained.

The methyl torsion, ν_{18}, had been reported[7] as occurring at 62 cm^{-1} in the liquid phase. The three-fold barrier and the structure obtained from the microwave data indicate that it should be observed near 134 cm^{-1} in the spectra of the vapor. It is observed at 129.2 cm^{-1} in the spectrum of the "light" vapor (Fig. 4A) and at 99.0 cm^{-1} in the spectra of the perdeutero compound (Fig. 4B). The shift factor, ν_H/ν_D = 1.305 is lower than should be expected if the torsion was not mixed with other normal modes.

The barrier to internal rotation of the methyl group, V_3, was calculated using a computer program similar to one described by Lewis et al.[26] The barrier for the CH_3 rotor is 1.15 kcal/mole and for the CD_2 rotor it is 1.19 kcal/mole. Both barriers are lower than that calculated by the microwave splitting method.

The Raman spectrum of methylchloroformate solid at 18.7°K is quite rich (Fig. 3B). It had been suggested previously[7] that the unit cell of methylchloroformate contained one molecule or that if it contained two molecules it should be considered centrosymmetric. Eight sharp lattice modes are apparent in the Raman spectrum below the lowest fundamental (ν_{18}, methyl torsion, 135 cm^{-1}). This number of lattice modes rules out the possibility of there being only one molecule per unit cell and also rules out the possibility of two molecules in a centrosymmetric unit cell. Crystal structure data remain unavailable for methylchloroformate but such

data would be of interest.

There are several apparent examples of crystal splitting evident in the spectrum, some of them quite striking. The pair of bands at 3028/3016 cm^{-1} had also been reported in the infrared study of the solid.[7] The authors reported an isotopic dilution study of this band pair from which they concluded the pair did not result from crystal splitting. Further examples in the Raman spectrum that apparently result from crystal splitting are ν_3, the carbonyl stretch (1774/1757/1752 cm^{-1}), ν_{12}, the COC in-plane bend (283/277 cm^{-1}), ν_{15}, the CH_3 rock (1152/1147 cm^{-1}) and ν_{17}, the methoxy torsion (194/182 cm^{-1}). These apparent examples of crystal splitting are quite reasonable in view of the crystal structure required by the large number of lattice modes evident in the Raman spectrum.

NUCLEAR MAGNETIC RESONANCE RESULTS

The proton decoupled ^{13}C NMR spectrum of $ClCO_2{}^{13}CH_3$ in 1,2-dibromo,tetrafluoroethane at 29°C consists of a single resonance with a half height linewidth ($\nu_{1/2}$) of 0.8 Hz. The spectrum was studied as a function of temperature to -105°C. Throughout the temperature range covered, there was no significant line-broadening observed.

The ^1H NMR spectrum of methylchloroformate in CS_2/CD_2Cl_2 (50/50) at 26°C consists of a single resonance with $\nu_{1/2}$ = 0.25 Hz. T_1 was measured to be 15 seconds. The spectrum was again studied as a function of temperature to -100°C. At -100°C, $\nu_{1/2}$ = 0.55 Hz and T_1 = 2.36 seconds. The small amount of apparent line-broadening observed at the lower temperature can be completely attributed to the change in T_1 and the fact that the magnetic field was more difficult to shim at -100°C because of the ^2H lock utilized on the Varian model XL-100. For these reasons the small apparent line-broadening in the ^1H NMR spectrum at -100°C should not be ascribed to any chemical exchange processes.[9]

CONCLUSIONS

The microwave spectrum of methylchloroformate has beer thoroughly reinvestigated. The data are interpreted to indicate that only one form of this molecule exists through, given the richness of the spectrum, small amounts of a second rotamer cannot positively be ruled out with these data alone. Further the microwave data are conclusively interpreted to demonstrate that the stable form of methylchloroformate is the s-trans form not the s-cis form as had been previously reported.[9] From this microwave study it has been possible to obtain the structural parameters of this stable form along with the dipole moment components.

The vibrational data include the first direct observation of the methyl torsion of gaseous methylchloroformate and that observation is consistent with the structure and barrier calculated from the rotational data. The Raman spectrum of the solid provides more specific data on which to base generalizations as to the crystal structure of methylchloroformate than the infrared spectrum of the solid alone[7] and again confirms the complimentary nature of the two sources of vibrational data.

The ^{13}C NMR temperature study is interpreted to be much more strongly suggestive of the likelihood that methylchloroformate has only one stable molecular conformation (s-trans) at room temperature and below. The ^{1}H NMR temperature study provided data that is felt to demonstrate the need for care in the performance and interpretation of such experiments.[9]

ACKNOWLEDGEMENT

The authors gratefully acknowledge the financial support given this study by the National Aeronautics and Space Administration through grant NGL-41-002-003. The authors also gratefully acknowledge the services of Dr. Paul Ellis and Mr. David Baily for providing the NMR data and the expertise necessary for their evaluation.

REFERENCES

†Taken from the thesis of M. G. Griffin which will be submitted to the Department of Chemistry in partial fulfillment of the Ph.D. degree.

1. S. Mizushima and M. Kubo, Bull. Chem. Soc. Jap. 13, 174 (1938).
2. R. J. W. LeFevre and A. Sundaram, J. Chem. Soc. (Lond.) 1962, 3904.
3. E. Bock and D. Iwacha, Can. J. Chem. 45, 3177 (1967).
4. M. J. Aroney, R. J. W. LeFevre, R. K. Pierens, and H. L. K. The, Aust. J. Chem. 22, 1599 (1969).
5. B. Collingwood, H. Lee, and J. K. Wilmshurst, Aust. J. Chem. 19, 1637 (1966).
6. R. A. Nyquist, Spectrochim. Acta 28A, 285 (1972).
7. J. E. Katon and M. G. Griffin, J. Chem. Phys. 59, 5868 (1973).
8. J. M. O'Gormm, W. Shand, Jr., and V. Schomaker, J. Amer. Chem. Soc. 72, 4222 (1950).
9. M. Oki and H. Nakanishi , Bull. Chem. Soc. Jap. 45, 1552 (1972).
10. A. J. Cohen and M. A. Whitehead, J. C. S. Faraday II, 68, 649 (1972).
11. D. G. Lister and N. L. Owen, J. C. S. Faraday II, 69, 1036 (1973).
12. W. Hentschel, Chem. Ber. 18, 1177 (1885).
13. R. Freeman and H. D. W. Hill, Jr., J. Chem. Phys., 53, 5103 (1970).
14. J. Kraitchman, Am. J. Phys. 21, 17 (1953).
15. T. Oka, J. Phys. Soc. Jap. 15, 2274 (1960).
16. G. W. Robinson, J. Chem. Phys. 21, 1741 (1953).
17. R. F. Curl, Jr., J. Chem. Phys 30, 1529 (1959).
18. G. H. Kwei, and R. F. Curl, Jr., J. Chem. Phys. 32, 1592 (1960).
19. C. C. Costain, and J. M. Jowling, J. Chem. Phys. 32 158 (1960).
20. O. H. LeBlanc, V. W. Laurie, and W. D. Gwinn, J. Chem. Phys. 33, 598 (1960).
21. W. Gordy, and R. L. Cook, Microwave Molecular Spectra (Wiley, New York, 1970) Chapt. 9.
22. J. R. Durig, K. L. Kizer, and Y. S. Li, J. Amer. Chem. Soc. 96, 7400 (1974).

23. G. Williams, N. L. Owen, and J. Sheridan, Trans. Faraday Soc. 67, 922 (1971).

24. J. S. Muenter, J. Chem. Phys., 48, 4544 (1968).

25. M. G. Griffin, "The Vibrational Assignment of Methylchloroformate", M. S. Thesis, Miami University, Oxford, Ohio, 1972.

26. J. D. Lewis, T. B. Malloy, Jr., T. H. Chao, and J. Laane, J. Mol. Struct. 12, 427 (1972).

Table I. The Microwave Spectra of Methylchloroformate

$^{35}Cl^{12}C^{16}O_2{}^{12}CH_3$

$J'_{k_{-1}k_{+1}} \leftarrow J_{k_{-1}k_{+1}}$	Observed	F'	←	F	Calculated	Obs-Calc	Unperturbed Level	A or E
$3_{03} \leftarrow 2_{02}$	14366.90	9/2	←	7/2	14366.76	0.14	14366.21	A
	14363.24	5/2	←	3/2	14363.12	0.12		A
$3_{13} \leftarrow 2_{12}$	13642.09	9/2	←	7/2	13641.94	0.15	13640.52	A
	13638.40	7/2	←	5/2	13638.22	0.18		A
$3_{12} \leftarrow 2_{11}$	15303.35	9/2	←	7/2	15303.29	0.06	15301.74	A
	15299.62	7/2	←	5/2	15299.57	0.05		A
$4_{04} \leftarrow 3_{03}$	19014.28	11/2+9/2	←	9/2+7/2	19014.14	0.14	19013.84	A
	19012.57	7/2+5/2	←	5/2+3/2	19012.39	0.18		A
$4_{14} \leftarrow 3_{13}$	18154.10	11/2	←	9/2	18153.98	0.12	18153.33	A
	18152.70	9/2	←	7/2	18152.51	0.19		A
	18152.15	7/2	←	5/2	18151.77	0.38		A
	18153.40	5/2	←	3/2	18153.24	0.16		A
$4_{13} \leftarrow 3_{12}$	20364.25	11/2	←	9/2	20363.94	0.31	20363.35	A
	20362.57	9/2	←	7/2	20362.48	0.09		A
	20362.11	7/2	←	5/2	20361.65	0.46		A
$4_{22} \leftarrow 3_{21}$	19605.73	11/2	←	9/2	19605.76	-0.03	19603.48	A
		9/2	←	7/2	19599.69			A
	19601.73	7/2	←	5/2	19601.80	-0.07		A
	19607.78	5/2	←	3/2	19607.87	-0.09		A
	19596.54	11/2	←	9/2			19594.42	E
	19590.72	9/2	←	7/2				E
	19592.80	7/2	←	5/2				E
		5/2	←	3/2				E

Table I Continued

$^{35}Cl\,^{12}C\,^{16}O_2\,^{12}CH_3$

$J'_{k'_{-1}k'_{+1}} \leftarrow J_{k_{-1}k_{+1}}$	Observed	F' ← F	Calculated	Obs-Calc	Unperturbed Level	A or E
$5_{05} \leftarrow 4_{04}$	23553.51	13/2 ← 11/2	23553.40	0.11	23553.25	A
	23552.58	9/2 ← 7/2	23552.48	0.10		A
$5_{15} \leftarrow 4_{14}$	22640.36	13/2 ← 11/2	22640.40	-0.04	22640.02	A
	22639.83	11/2 ← 9/2	22639.68	0.15		A
	22639.41	9/2 ← 7/2	22639.03	0.38		A
$5_{14} \leftarrow 4_{13}$	25387.83	13/2 ← 11/2	25388.02	-0.19	25387.24	A
	25387.02	11/2 ← 9/2	25387.32	-0.30		A
$5_{24} \leftarrow 4_{23}$	24082.85	13/2 ← 11/2	24082.75	0.10	24081.70	A
	24080.12	11/2 ← 9/2	24079.78	0.34		A
	24084.85	13/2 ← 11/2			24083.74	E
	24082.19	11/2 ← 9/2				E
$5_{23} \leftarrow 4_{22}$	24680.69	13/2 ← 11/2	24680.41	0.28	24679.45	A
	24677.75	11/2 ← 9/2	24677.32	0.43		A
	24678.69	13/2 ← 11/2			24677.54	E
	24675.94	11/2 ← 9/2				E
$6_{06} \leftarrow 5_{05}$	27981.37	15/2 ← 13/2	27981.36	0.01	27981.18	A
	27980.77	11/2 ← 9/2	27980.78	-0.01		A
$6_{16} \leftarrow 5_{15}$	27098.04	15/2 ← 13/2	27098.08	-0.01	27097.80	A
	27097.79	13/2 ← 11/2	27097.68	0.11		A
	27097.33	11/2 ← 9/2	27097.18	0.15		A
$6_{15} \leftarrow 5_{14}$	30361.85	15/2 ← 13/2	30361.83	0.02	30361.54	A
	30361.49	13/2 ← 11/2	30361.46	0.03		A
	30361.08	11/2 ← 9/2	30360.92	0.16		A

Table I Continued

$^{35}Cl^{12}C^{16}O_2{}^{12}CH_3$

$J'_{k'_{-1}k'_{+1}} \leftarrow J_{k_{-1}k_{+1}}$	Observed	F'	←	F	Calculated	Obs-Calc	Unperturbed Level	A or E
$6_{25} \leftarrow 5_{24}$	28841.62	15/2	←	13/2	28841.50	0.12	28840.82	A
	28839.95	13/2	←	11/2	28839.82	0.13		A
	28842.29	15/2	←	13/2			28841.49	E
	28840.62	13/2	←	11/2				E
$6_{24} \leftarrow 5_{23}$	29840.51	15/2	←	13/2	29840.42	0.09	29839.65	A
	29838.72	13/2	←	11/2	29838.09	0.03		A
	29839.98	15/2	←	13/2			29839.14	E
	29838.23	13/2	←	11/2				E
$7_{07} \leftarrow 6_{06}$	32313.35	17/2	←	15/2	32313.31	0.04	32313.17	A
	32312.99	13/2	←	11/2	32312.92	0.07		A
	32312.66	11/2	←	9/2	32312.81	-0.15		A
$7_{17} \leftarrow 6_{16}$	31526.02	17/2	←	15/2	31526.06	-0.04	31525.78	A
	31525.75	15/2	←	13/2	31525.82	-0.07		A
	31525.48	13/2	←	11/2	31525.43	0.05		A
$7_{16} \leftarrow 6_{15}$	35269.20	17/2	←	15/2	35269.35	-0.15		A
	35269.01	15/2	←	13/2	35269.15	-0.14	35269.03	A
	35268.82	13/2	←	11/2	35268.93	-0.11		A
$7_{26} \leftarrow 6_{25}$	33529.92	17/2	←	15/2	33569.88	0.04	33569.38	A
	33568.91	15/2	←	13/2	33568.85	0.06		A
$7_{25} \leftarrow 6_{24}$	35064.18	17/2	←	15/2	35064.29	-0.11	35063.55	A
	35062.98	15/2	←	13/2	35063.15	-0.17		A
$7_{34} \leftarrow 6_{33}$	34143.18	17/2	←	15/2	34143.41	-0.23	34142.13	A
	34140.89	15/2	←	13/2	34140.96	-0.07		A
	34143.55	11/2	←	9/2	34143.73	-0.18		A

Table I Continued

$^{35}Cl^{12}C^{16}O_2{}^{12}CH_3$

$J'_{k'_{-1}k'_{+1}} \leftarrow J_{k_{-1}k_{+1}}$	Observed	F'	←	F	Calculated	Obs-Calc	Unperturbed Level	A or E
$8_{08} \leftarrow 7_{07}$	36578.20	19/2	←	17/2	36578.36	-0.16	36578.11	A
	36577.99	15/2	←	13/2	56578.07	-0.08		A
	36577.79	13/2	←	11/2	36577.99	-0.20		A
$8_{18} \leftarrow 7_{17}$	35924.89	19/2	←	17/2	35925.15	-0.26	35924.70	A
	35924.75	17/2	←	15/2	35924.96	-0.21		A
$8_{17} \leftarrow 7_{16}$	40092.32	19/2	←	17/2	40092.53	-0.21	40092.09	A
	40092.07	17/2	←	15/2	40092.44	-0.37		A
	40091.87	15/2	←	13/2	40092.10	-0.23		A
$8_{27} \leftarrow 7_{26}$	38263.35	19/2	←	17/2	38263.48	-0.13	38263.00	A
	38262.77	17/2	←	15/2	38262.81	-0.04		A
$6_{16} \leftarrow 5_{05}$	31148.83	15/2	←	13/2	31148.73	0.10	31149.07	A
	31150.00	13/2	←	11/2	31149.86	0.14		A
	31147.90	9/2	←	7/2	31147.80	0.10		A
	31146.81	15/2	←	13/2			31147.00	E
	31147.90	13/2	←	11/2				E
	31145.80	9/2	←	7/2				E
$7_{17} \leftarrow 6_{06}$	34693.44	17/2	←	15/2	34693.41	0.03	34693.55	A
	34694.18	15/2	←	13/2	34694.19	-0.01		A
	34692.74	11/2	←	9/2	34692.78	-0.04		A
	34691.56	17/2	←	15/2			34691.72	E
	34692.36	15/2	←	13/2				E
	34690.93	11/2	←	9/2				E

Table I Continued

$^{35}Cl\,^{12}C\,^{16}O_2\,^{12}CH_3$

$J'_{k'_{-1}k'_{+1}} \leftarrow J_{k_{-1}k_{+1}}$	Observed	F' ← F	Calculated	Obs-Calc	Unperturbed Level	A or E
$8_{18} \leftarrow 7_{07}$	38305.20	19/2 ← 17/2	38305.24	-0.04	38305.27	A
	38305.68	17/2 ← 15/2	38305.77	-0.09		A
	38304.74	13/2 ← 11/2	38304.79	-0.05		A
	38303.58	19/2 ← 17/2			38303.61	E
	38304.01	17/2 ← 15/2				E
	38303.06	13/2 ← 11/2				E

$^{37}Cl\,^{12}C\,^{16}O_2\,^{12}CH_3$

$3_{03} \leftarrow 2_{02}$	14034.80	9/2+7/2 ← 7/2+5/2	14034.77	0.03	14034.24	A
	14031.90	5/2+3/2 ← 3/2+1/2	14031.87	0.03		A
$6_{06} \leftarrow 5_{05}$	27377.36	13/2 ← 11/2	27377.32	0.04	27377.03	A
	27377.07	15/2 ← 13/2	27377.18	-0.09		A
$6_{16} \leftarrow 5_{15}$	26502.95	15/2 ← 13/2	26502.90	0.05	26502.68	A
	26502.64	13/2 ← 11/2	26502.60	0.04		A
$6_{15} \leftarrow 5_{14}$	29630.17	15/2+13/2 ← 13/2+11/2	29630.10	0.07	29630.03	A
$6_{24} \leftarrow 5_{23}$	29085.75	15/2 ← 13/2	29085.63	0.12	29085.07	A
	29084.33	13/2 ← 11/2	29084.19	0.14		A
	29085.10	15/2 ← 13/2			29084.50	E
	29083.84	13/2 ← 11/2				E
$7_{07} \leftarrow 6_{06}$	31629.18	15/2 ← 13/2	31629.10	0.08	31628.94	A
	31629.00	17/2 ← 15/2	31628.97	0.03		A
$7_{17} \leftarrow 6_{16}$	30838.25	17/2+15/2 ← 15/2+13/2	30838.27	-0.02	30838.15	A

Table I Continued

$^{37}Cl\,^{12}C\,^{16}O_2\,^{12}CH_3$

$J'_{k'_{-1}k'_{+1}} \leftarrow J_{k_{-1}k_{+1}}$	Observed	F' ← F	Calculated	Obs-Calc	Unperturbed Level	A or E
$7_{16} \leftarrow 6_{15}$	34430.71	17/2+15/2←15/2+13/2	34430.70	0.01	34430.59	A
$7_{25} \leftarrow 6_{24}$	34170.53	17/2 ← 15/2	34170.54	-0.01	34170.04	A
	34169.60	19/2 ← 17/2	34169.62	-0.02		A
$8_{08} \leftarrow 7_{07}$	35813.41	15/2 ← 13/2	35813.40	0.01	35813.22	A
	35813.24	17/2 ← 15/2	35813.28	-0.04		A
$8_{18} \leftarrow 7_{17}$	35146.57	19/2 ← 17/2	35146.64	-0.07	35146.44	A
	35146.48	17/2 ← 15/2	35146.54	-0.06		A
$8_{17} \leftarrow 7_{16}$	39155.34	19/2+17/2←17/2+15/2	39155.41	-0.07	39155.24	A
$8_{27} \leftarrow 7_{26}$	37382.34	19/2 ← 17/2	37382.34	0.00	37382.06	A
	37381.88	17/2 ← 15/2	37381.83	0.05		A
$8_{26} \leftarrow 7_{25}$	39287.67	19/2 ← 17/2	39287.78	-0.11	39287.31	A
	39287.10	17/2 ← 15/2	39287.16	-0.06		A

$^{35}Cl\,^{12}C\,^{16}O_2\,^{12}CD_3$

$6_{06} \leftarrow 5_{05}$	25500.25	15/2 ← 13/2	25500.18	0.07	25500.09	A
	25499.72	11/2 ← 9/2	25499.63	0.09		A
$6_{15} \leftarrow 5_{14}$	27398.40	15/2 ← 13/2	27398.34	0.06	27398.08	A
	27397.99	13/2+9/2←11/2+7/2	27397.90	0.09		A
	27397.59	11/2 ← 9/2	27397.46	0.13		A
$6_{25} \leftarrow 5_{24}$	26128.59	15/2 ← 13/2	26128.51	0.09	26127.84	A
	26127.04	13/2+11/2←11/2+9/2	26126.91	0.11		A

Table I Continued

$^{35}Cl^{12}C^{16}O_2{}^{12}CD_3$

$J'_{k'_{-1}k'_{+1}} \leftarrow J_{k_{-1}k_{+1}}$	Observed	F' ← F	Calculated	Obs-Calc	Unperturbed Level	A or E
$6_{24} \leftarrow 5_{23}$	26855.95	15/2 ← 13/2	26855.88	0.07	26855.12	A
	26854.23	13/2 ← 11/2	26854.18	0.05		A
$7_{07} \leftarrow 6_{06}$	29494.20	17/2 ← 15/2	29494.17	0.03	29494.02	A
	29493.77	15/2+13/2←13/2+11/2	29493.63	0.14		A
$7_{17} \leftarrow 6_{15}$	31858.88	17/2 ← 15/2	31858.92	-0.04	31858.67	A
	31858.70	15/2 ← 13/2	31858.72	-0.02		A
	31858.53	11/2 ← 9/2	31858.52	0.01		A
	31858.32	13/2 ← 11/2	31858.32	0.00		A
$7_{26} \leftarrow 6_{25}$	30426.94	17/2 ← 15/2	30427.02	-0.08	30426.42	A
	30425.91	15/2+13/2←13/2+11/2	30425.98	-0.07		A
$7_{25} \leftarrow 6_{24}$	31530.17	17/2 ← 15/2	31530.23	-0.06	31529.60	A
	31529.03	15/2+13/2←13/2+11/2	31529.08	-0.05		A
$7_{34} \leftarrow 6_{33}$	30829.38	17/2 ← 15/2	30829.49	-0.11	30828.38	A
	30827.08	15/2 ← 13/2	30827.18	-0.10		A
$6_{16} \leftarrow 5_{05}$	28881.94	13/2 ← 11/2	28881.95	-0.01	28881.03	A
	28880.78	15/2 ← 13/2	28880.79	-0.01		A

$^{35}Cl^{12}C^{16}O_2{}^{13}CH_3$

$4_{04} \leftarrow 3_{03}$	18566.43	11/2+9/2 ←9/2+7/2	18566.42	0.01	18565.98	A
	18564.72	7/2+5/2 ←5/2+3/2	18564.74	-0.02		A
$5_{05} \leftarrow 4_{04}$	23011.96	13/2+11/2←11/2+9/2	23012.01	-0.05	23011.65	A
	23011.03	9/2+7/2 ← 7/2+5/2	23011.01	0.02		A

Table I Continued

$^{35}Cl\,^{12}C\,^{16}O_2\,^{13}CH_3$

$J'_{k'_{-1}k'_{+1}} \leftarrow J_{k_{-1}k_{+1}}$	Observed	F' ← F	Calculated	Obs-Calc	Unperturbed Level	A or E
$6_{25} \leftarrow 5_{24}$	28140.95	15/2+9/2 ← 13/2+7/2	28140.90	0.05	28140.16	A
	28139.31	13/2+11/2← 11/2+9/2	28139.30	0.01		A
	28141.67	15/2+9/2 ← 13/2+7/2			28140.88	E
	28140.02	13/2+11/2← 11/2+9/2				E
$6_{24} \leftarrow 5_{23}$	29054.61	15/2+9/2 ← 13/2+7/2	29054.53	0.08	29053.74	A
	29052.79	13/2+11/2← 11/2+9/2	29052.78	0.01		A
	29053.99	15/2+9/2 ← 13/2+7/2			29053.16	E
	29052.26	13/2+11/2← 11/2+9/2				E
$7_{26} \leftarrow 6_{25}$	32759.63	17/2+11/2← 15/2+9/2	32759.64	-0.01	32759.19	A
	32758.69	15/2+13/2← 13/2+11/2	32758.66	0.03		A
$7_{25} \leftarrow 6_{24}$	34133.36	17/2+11/2← 15/2+9/2	34133.46	-0.10	34132.88	A
	34132.30	15/2+13/2← 13/2+11/3	34132.33	-0.03		A
$8_{18} \leftarrow 7_{07}$	37646.46	17/2 ← 15/2	37646.63	-0.17	37646.14	A
	37646.12	19/2+15/2← 17/2+13/2	37646.10	0.02		A
	37645.69	13/2 ← 11/2	37645.55	0.14		A

$^{35}Cl\,^{12}C\,^{16}O_2\,^{12}CH_2D$-OOP

$3_{03} \leftarrow 2_{02}$	13923.95	9/2+7/2← 7/2+5/2	13923.88	0.07	13923.22	A
	13920.26	5/2+3/2← 3/2+1/2	13920.24	0.02		A
$3_{12} \leftarrow 2_{11}$	14783.69	9/2+3/2← 7/2+1/2	14783.50	0.19	14782.06	A
	14780.00	7/2+5/2← 5/2+3/2	14799.86	0.14		A

Table I Continued

$^{35}Cl^{12}C^{16}O_2{}^{12}CH_2D$-OOP

$J'_{k'_{-1}k'_{+1}} \leftarrow J_{k_{-1}k_{+1}}$	Observed	F' ← F	Calculated	Obs-Calc	Unperturbed Level	A or E
$4_{04} \leftarrow 3_{03}$	13923.95	9/2+7/2 ← 7/2+5/2	13923.88	0.07	13923.22	A
	18440.64	7/2+5/2 ← 5/2+3/2	18440.64	0.00		A
$4_{14} \leftarrow 3_{13}$	17632.27	11/2 ← 9/2	17632.31	-0.04	17631.45	A
	17631.54	5/2 ← 3/2	17631.55	-0.01		A
	17630.83	9/2 ← 7/2	17630.86	-0.03		A
	17630.19	7/2 ← 5/2	17630.10	0.09		A
$4_{13} \leftarrow 3_{12}$	19676.46	11/2 ← 9/2	19676.52	-0.06	19675.65	A
	19675.62	5/2 ← 3/2	19675.74	-0.12		A
	19675.13	9/2 ← 7/2	19675.08	0.05		A
	19674.41	7/2 ← 5/2	19674.30	0.11		A
$5_{05} \leftarrow 4_{04}$	22865.86	13/2+11/2 ← 11/2+9/2	22865.86	0.00	22865.56	A
	22864.88	9/2+11/2 ← 7/2+5/2	22864.84	0.04		A
$5_{14} \leftarrow 4_{13}$	24538.20	13/2 ← 11/2	24538.28	-0.08	24537.72	A
	24537.62	11/2+7/2 ← 9/2+5/2	24537.60	0.02		A
	24536.92	9/2 ← 7/2	24536.91	0.01		A
$5_{24} \leftarrow 4_{23}$	23325.99	13/2+7/2 ← 11/2+5/2	23326.04	-0.05	23324.54	A
	23323.10	11/2+9/2 ← 9/2+7/2	23323.12	-0.02		A
$8_{18} \leftarrow 7_{07}$	37471.78	17/2 ← 15/2	37471.73	0.05	37471.34	A
	37471.29	19/2 ← 17/2	37471.28	0.01		A
	37470.81	13/2 ← 11/2	37470.85	-0.04		A

Table I Continued

$^{35}Cl^{12}C^{16}O_2{}^{12}CH_2D$-IP

$J'_{k'_-k'_+} \leftarrow J_{k_-k_+}$	Observed	F' ← F	Calculated	Obs-Calcd	Unperturbed Level	A or E
$3_{12} \leftarrow 2_{11}$	14686.41	9/2 ← 7/2	14686.29	0.12	14684.90	A
	14682.92	7/2←5/2←5/2←3/2	14682.61	0.31		A
$6_{15} \leftarrow 5_{14}$	29144.92	15/2 ← 13/2	29144.83	0.09	29144.66	A
	29144.56	13/2 ← 11/2	29144.44	0.12		A
	29144.23	11/2 ← 9/2	29143.93	0.30		A
$6_{24} \leftarrow 5_{23}$	28628.59	5/2←9/2←3/2←7/2	28628.54	0.05	28627.74	A
	28626.87	13/2←11/2←11/2←9/2	28626.81	0.06		A
$6_{25} \leftarrow 5_{24}$	27693.97	15/2←9/2←13/2←7/2	27694.00	-0.03	27693.20	A
	27692.38	13/2←11/2←11/2←9/2	27692.34	0.04		A
$7_{25} \leftarrow 6_{24}$	33637.46	17/2←11/2←15/2←9/3	33637.45	0.01	33636.96	A
	33636.40	15/2←13/2←13/2←11/3	33636.37	0.03		A
$7_{26} \leftarrow 6_{25}$	32236.10	17/2←11/2←15/2←9/2	32236.12	-0.02	32235.60	A
	32235.17	15/2←13/2←13/2←11/2	32235.11	0.06		A
$8_{26} \leftarrow 7_{25}$	38675.55	19/2←13/2←17/2←11/2	38675.60	-0.05	38675.24	A
	38674.86	17/2←15/2←(15/2←13/2	38674.92	-0.06		A
$8_{27} \leftarrow 7_{26}$	36745.89	19/2←13/2←13/2←11/2	36745.98	-0.09	36745.57	A
	36745.19	17/2←15/2←15/2←13/3	36745.30	-0.11		A
$7_{17} \leftarrow 6_{06}$	33426.72	15/2 ← 13/2	33426.76	-0.07	33426.23	A
	33426.19	17/2 ← 15/2	33426.11	0.08		A
$8_{18} \leftarrow 7_{07}$	36889.70	17/2 ← 15/2	36889.72	-0.02	36889.31	A
	36889.25	19/2←15/2←17/2←13/2	36889.29	-0.04		A
	36888.81	13/2 ← 11/2	36888.86	-0.05		A

TABLE II. Rotational constants, moments of inertia and nuclear quadrupole coupling constants for metnylchloroformate

	$^{35}Cl^{12}C^{16}O_2{}^{12}CH_3$	$^{37}Cl^{12}C^{16}O_2{}^{12}CH_3$	$^{35}Cl^{12}C^{16}O_2{}^{12}CD_3$	$^{35}Cl^{12}C^{16}O_2{}^{13}CH_3$	$^{35}Cl^{12}C^{16}O_2{}^{12}CH_2D$-OOP	$^{35}Cl^{12}C^{16}O_2{}^{12}CH_2D$-IP
A	9765.82 ± 0.20	9738.39 ± 0.29	9172.25 ± 0.18	9738.40 ± 0.30	9619.16 ± 0.15	9465.36 ± 0.30
B	2692.17 ± 0.01	2623.00 ± 0.01	2413.68 ± 0.01	2620.09 ± 0.01	2594.66 ± 0.01	2582.49 ± 0.01
C	2138.03 ± 0.01	2092.92 ± 0.01	1957.65 ± 0.01	2091.18 ± 0.01	2082.27 ± 0.01	2054.86 ± 0.01
I_a	51.7498 ± 0.0011	51.8955 ± 0.0016	55.0987 ± 0.0011	51.8955 ± 0.0016	52.5388 ± 0.0009	53.3925 ± 0.001
I_b	187.722 ± 0.001	192.671 ± 0.001	209.381 ± 0.001	192.886 ± 0.001	194.777 ± 0.001	195.694 ± 0.001
I_c	236.376 ± 0.001	241.471 ± 0.001	258.156 ± 0.001	241.672 ± 0.001	242.706 ± 0.001	245.943 ± 0.001
Δ	3.096	3.097	6.324	3.110	4.610	
χ_{aa}	-59.8 ± 0.5	046.4 ± 0.5	-56.7 ± 0.5	-57.2 ± 0.5	-58.6 ± 0.5	-56.2 ± 0.5
χ_{bb}	31.2 ± 1.0	25.4 ± 1.0	29.8 ± 1.0	30.9 ± 1.0	29.7 ± 1.0	29.6 ± 1.0
χ_{cc}	28.6 ± 1.0	21.0 ± 1.0	26.9 ± 1.0	26.3 ± 1.0	28.9 ± 1.0	26.6 ± 1.0

TABLE III

Coordinates of the atoms for which isotopic substitutions were made[a]

	Chlorine	Carbon (methyl)	Hydrogen (in plane)	Hydrogen (out of plane)
X	-1.590	2.278	2.808	2.510
Y	-0.278	-0.381	-1.312	0.182
Z	0.014[b]	0.084[b]	0.161[b]	±0.887

[a]Error limits on the coordinates are never worse than ±0.005.

[b]The Z-coordinate of these atoms was taken as 0.0 for subsequent calculations.

TABLE IV

Coordinates of the unsubstituted atoms calculated from the moment relations

	Carbon (carbonyl)	Oxygen (carbonyl)	Oxygen (ether)
X	0.034[a]	0.353	0.895
Y	0.312	1.458	-0.740
Z	0.0[b]	0.0[b]	0.0[b]

[a]This value was chosen so that the carbonyl bond length would equal 1.190 Å.

[b]These values were assumed based on a consideration of the inertial defect.

TABLE V

Structural parameters for methylchloroformate[a]

	Bond Lengths (Å)	Bond Angles (°)	
Cl-C	1.73	Cl-C=O	126
C=O	1.19	O=C-O	125
(O=)C-O	1.36	C-O-C	115
O-C(H_3)	1.43	O-C-H(IP)	105
C-H(IP)	1.07	O-C-H(OOP)	110
C-H(OOP)	1.08	H-C-H(OOP-OOP)	111
		H-C-H(IP-OOP)	110

[a]Calculated from the coordinates in Table III and IV. The errors associated with these parameters because of the assumptions involved in their calculation are probably no worse than ±0.02 Å for the bond lengths and ±2° for the bond angles.

TABLE VI

Internal rotation splitting (MHz) and parameters of methylchloroformate

	^{35}Cl ^{12}C $^{16}O_2$ $^{12}CH_3$		^{37}Cl ^{12}C $^{16}O_2$ $^{12}CH_3$		^{35}Cl ^{12}C $^{16}O_2$ $^{13}CH_3$	
Transition	$\nu_E-\nu_A$	V_3 (cal/mol)	$\nu_E-\nu_A$	V_3 (cal/mol)	$\nu_E-\nu_A$	V_3 (cal/mol)
$4_{22} \leftarrow 3_{21}$	-9.06	1190				
$5_{24} \leftarrow 4_{23}$	2.04	1230				
$5_{23} \leftarrow 4_{22}$	-1.91	1240				
$6_{25} \leftarrow 5_{24}$	0.67	1230			0.72	1230
$6_{24} \leftarrow 5_{23}$	-0.51	1270	-0.57	1270	-0.58	1270
$6_{16} \leftarrow 5_{05}$	-2.09	1220				
$7_{17} \leftarrow 6_{06}$	-1.83	1220				
$8_{18} \leftarrow 7_{07}$	-1.66	1220				

I_α	2.954 amu · Å^2	2.954 amu · Å^2	2.955 amu · Å^2
F	171.1 GH_3	171.1 GH_3	171.0 GH_3
α	0.05598	0.05945	0.05926
β	0.00432	0.00439	0.00456
γ	0.0	0.0	0.0
V_3	1230 ± 30 cal/mol		

TABLE VII

Stark coefficients [(MHz cm^2)/V^2] and dipole moments of methylchloroformate[a]

Transition	|M|	$\Delta\nu/E^2$ ($X10^5$)	
		Obsd.	Calcd.
$5_{05} \leftarrow 4_{04}$	0	0.09	0.07
	3	0.28	0.41
	4	0.59	0.67

$|\mu_a| = 1.7 \pm 0.2$
$|\mu_b| = 1.0 \pm 0.2$
$|\mu_c| = 0.0$[a]
$|\mu_t| = 2.0 \pm 0.2$

a.) By symmetry

Table VIII. The Vibrational Spectra and Assignment of Methylchloroformate

Vapor				Solid						Assignment
Infrared[a]		Raman		Infrared[a,b]				Raman[c]		
				A'		A"				
cm^{-1}	type	Δcm^{-1}	Rel Int	cm^{-1}	Rel Int	cm^{-1}	Rel Int	Δcm^{-1}	Rel Int	
				3976	vvw[d]	3976	w			A" $\nu_8 + \nu_{13}$ (3970)
				3904	vw					A' $\nu_2 + \nu_8$ (3914)
3571	AB			3509	w					A' $2\nu_3$ (3500)
3569				3491	m					
								3251	vvw	A" $\nu_1 + \nu_{17}$ (3253)
								3232	vvw	A'/A" $\nu_3 + \nu_4/\nu_{14}$ (3232)
								3207	vvw	A'/A" $\nu_3 + \nu_4/\nu_{14}$ (3207)
								3072	vvw	
3057		3047	w,p	3048	w	3048	vvw	3055	m	A' ν_1 CH_3 asymmetric stretch
3033	AC	∿3025	w,dp	3025	w	3025	s	3028	m	A" ν_{13} CH_3 asymmetric stretch
3016				3016	s	3016	s	3018	w	
3005										
				2978	sh					
2979										
2973	A	2962	vs,p	2961	s	2961	w	2963	vvs	A' ν_2 CH_3 symmetric stretch
2967		2934	p							
2920				2919	w			2914		
		2905	p	2902	w			to	vw,b	A' $2(\nu_4/\nu_{14})$ F.R. $\bar{w}$ ν_2
						2881	w	2880		
				2879	w					
2863				2869	w					
2855	A	2845	p	2846	ms	2846	w	2845	m	A' 2 ν_5 F.R. $\bar{w}$ ν_2
2849										

Table VIII. Con't.

Vapor				Solid						Assignment
Infrared[a]		Raman		Infrared[a,b] A'		Infrared[a,b] A"		Raman[c]		
cm^{-1}	type	Δcm^{-1}	Rel Int.	cm^{-1}	Rel Int	cm^{-1}	Rel Int	Δcm^{-1}	Rel Int	
								2640	vvw	
2610	?			2601	w			∿2603	vvw	A' $\nu_3 + \nu_9$ (2599)
				2582	w			∿2592	vvw	
				2570	w	2570	w	2577	vw	A' $2\nu_6$ (2578)
				2418	w					
2402				2406	w					A' $2\nu_7$ (2408)
				2371	vw					A'
				2316	m	2316	m			A' $2\nu_{15}$ (2304)
								2297	vw	A' $2\nu_{15}$ (2296)
								2273	vw	A'/A" $\nu_4/\nu_{14} + \nu_9$ (2271)
								2178	w	A' $\nu_3 + \nu_{11}$ (2183)
				2142	w					
								2120	vvw	A' $\nu_7 + \nu_8$ (2116)
				2095	w			∿2100	vvvw	A" $\nu_8 + \nu_{15}$(2099)
				2089	w			2079	vvw	
2027				2025	vw					A' $\nu_7 + \nu_9$ (2025)
2022										
1973	?			1960	vw					A" $\nu_3 + \nu_{17}$ (1956)
1924				1905	w					
				1890	w					A' $2\nu_8$ (1894)
				1882	ms			∿1880	vvw	

Table VIII. Con't.

Vapor				Solid						Assignment
Infrared[a]		Raman		Infrared[a,b]				Raman[c]		
				A'		A"				
cm^{-1}	type	Δcm^{-1}	Rel Int	cm^{-1}	Rel Int	cm^{-1}	Rel Int	Δcm^{-1}	Rel Int	
1806 1794 1788	B	1801 1792	p p	1789 to 1755	s			1774 1757 1752	w mw m	ν_3 C=O stretch
				1725	m					
				1716	s			1717	vw	A' $\nu_{12} + \nu_5$ (1717)
				1646	mw			1652	vw	A' $2\nu_9$ (1642)
				1622	mw			~1625	vw	A' $\nu_{14} + \nu_{17}$ (1622)
1464 1459 1448	?	1466 1459	p dp	1448.6	s	1449.2	s	1458 1450	m mw	A'/A" ν_4/ν_{14} CH_3 asymmetric deformation
1441 1433	?									
				1431	s	1431	sh	1432	mw	A' ν_5 CH_3 symmetric deformation
1396								~1405	vvw	
1382	?	1389	p	1387	s	1387	vw			A' $2\nu_{16}$ (1378)
				1326	mw					A' $\nu_{15} + \nu_{17}$ (1322)
1313 1308 1300	AB			1306 1297	s s	1306	w			A' $\nu_9 + \nu_{10}$ (1302) A' $\nu_9 + \nu_{10}$ (1296)

Table VIII. Con't.

Vapor				Solid						Assignment
Infrared[a]		Raman		Infrared[a,b]				Raman[c]		
				A'		A"				
cm^{-1}	type	Δcm^{-1}	Rel Int	cm^{-1}	Rel Int	cm^{-1}	Rel Int	Δcm^{-1}	Rel Int	
1233				1250		1250	w			
1210	?			to	s	1226	vw			
1202		1157	p	1210		1211	vw	1204	mw	A' ν_6 COC asymmetric stretch
1196										
				1186	s	1180	w			
1162	AB			1174	s			1169	mw	A' ν_7 CH_3r.
1154		1124	dp	1152	sh	1152	ms	1152	w	A" ν_{15} CH_3 r.
				1142	m	1142	w	1148	w	A" $\nu_9 + \nu_{17}$ (1141)
								1144	sh	
1060								1087	vvvw	
								1056	vvvw	
1036								1046	vvvw	
1007										
								988	vw	A' $\nu_{16} + \nu_{17}$ (985)
				961	w			972	vw	A' $2\nu_{10}$ (972)
				958	w			960	vw	A' $2\nu_{10}$ (958)
971		977	p					951	sh	A" $\nu_9 + \nu_{18}$ (956)
966	?	962	p	947	s	947	w	947	m	A' ν_8 COC symmetric stretch
957								932	vvw	
								924	vvw	
				920	w			918	vvw	
892				889	mw			~893	vvw	A' $\nu_{10} + \nu_{11}$ (895)

Table VIII. Con't.

Vapor				Solid						Assignment
Infrared[a]		Raman		Infrared[a,b]				Raman[c]		
				A'		A"				
cm^{-1}	type	Δcm^{-1}	Rel Int	cm^{-1}	Rel Int	cm^{-1}	Rel Int	Δcm^{-1}	Rel Int	
882				881	w					
830										
824	A	823	p	825	s	825	w			
816				821	s	821	w	821	ms	A' ν_9 C-Cl stretch
				817	ms					
				758	w			766	vw	
706										
694	C			689	w	689	s	702	vvvw	A" ν_{16} C-Cl bend
677				672	w	672	m			
668										
542										
527								518	vvvw	
494										
488	A	487	p	481	s	481	vw	486	vs	A' ν_{10} OCO bend
477		480	p	477	m	477	vw	479	ms	
		472	p							
413										
405	AB	406	p	407	s	407	w	409	ms	A' ν_{11} C-Cl bend
397										
								392	vvw	A' $2\nu_{17}$ (388)
354								367	vvw	A' $2\nu_{17}$ (364)

Table VIII. Con't.

Vapor				Solid					Assignment
Infrared[a]		Raman		Infrared[a,b]				Raman[c]	
				A'		A"			
cm^{-1}	type	Δcm^{-1}	Rel Int	cm^{-1}	Rel Int	cm^{-1}	Rel Int	Δcm^{-1}	Rel Int	
325								341	vvvw	
314	?									
304										
								283	w	
279	?	274	p	270	s			277	w	A' ν_{12} COC bend
268										
		Methylchloroformate-d_3								
		Infrared Vapor						202	vw	
163.2	s	148.8	s					194	w	
		148.2	s					182	w	A" ν_{17} Methoxy torsion
129.2	w	99.0	w					135	vvw	A" ν_{18} Methyl torsion
								122	ms	Lattice mode
								100	sh	Lattice mode
								94	s	Lattice mode
								81	w	Lattice mode
								67	mw	Lattice mode
								60	w	Lattice mode
								52	mw	Lattice mode
								45	m	Lattice mode

a.) Taken from Ref. 2
b.) Recorded at ~77°K
c.) Recorded at 187°K
d.) vw = very weak, w = weak, m = medium, s = strong, vs = very strong, b = broad, p = polarized, dp = depolarized

FIGURE CAPTIONS

Fig. 1 Possible conformations of methylchloroformate.

Fig. 2 The structure of methylchloroformate in the principal axis system.

Fig. 3 The Raman spectra of methylchloroformate. [A] The room temperature vapor. [B] The solid at 18.7°K.

Fig. 4 The far infrared spectra of [A] methylchloroformate and [B] methylchloroformate-d_3. Transitions marked with arrows correspond to a small amount of HCl impurity.

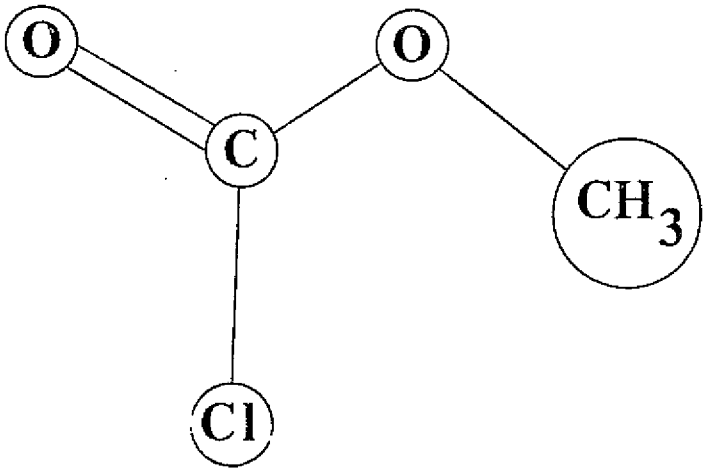

S - CIS

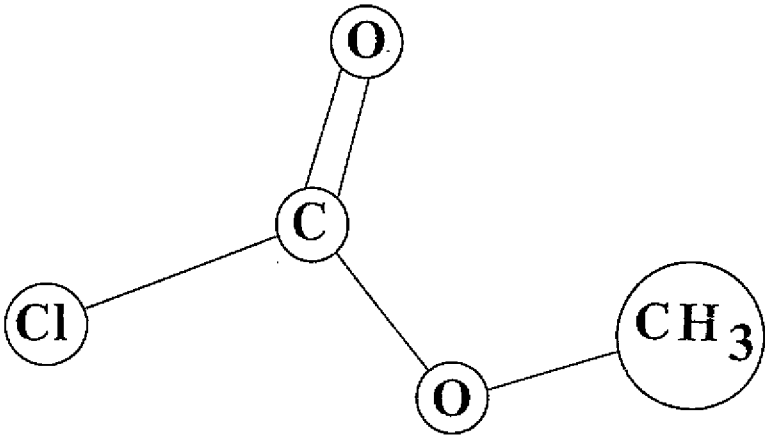

S-TRANS

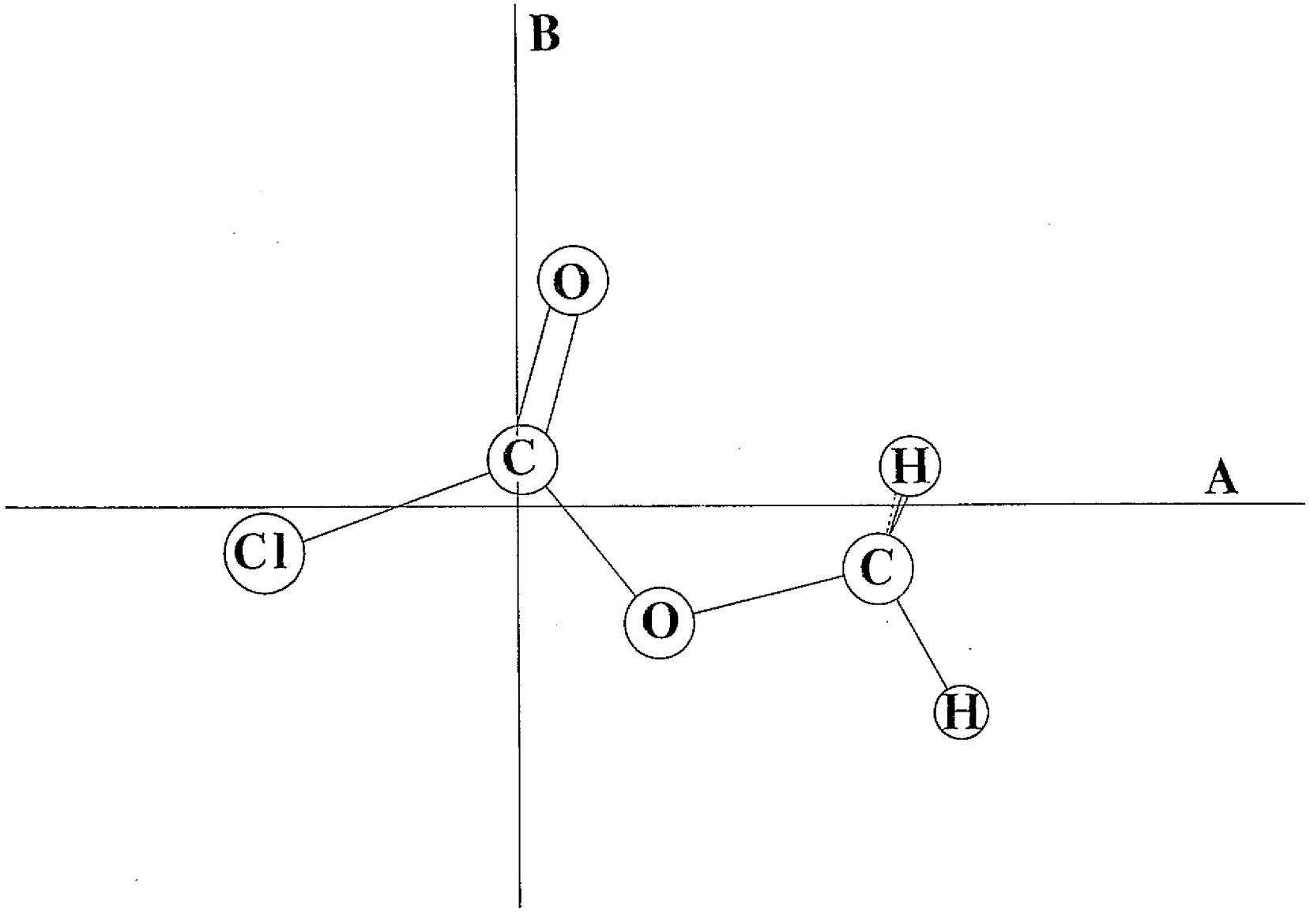
B
A
O
C
H
Cl
C
O
H

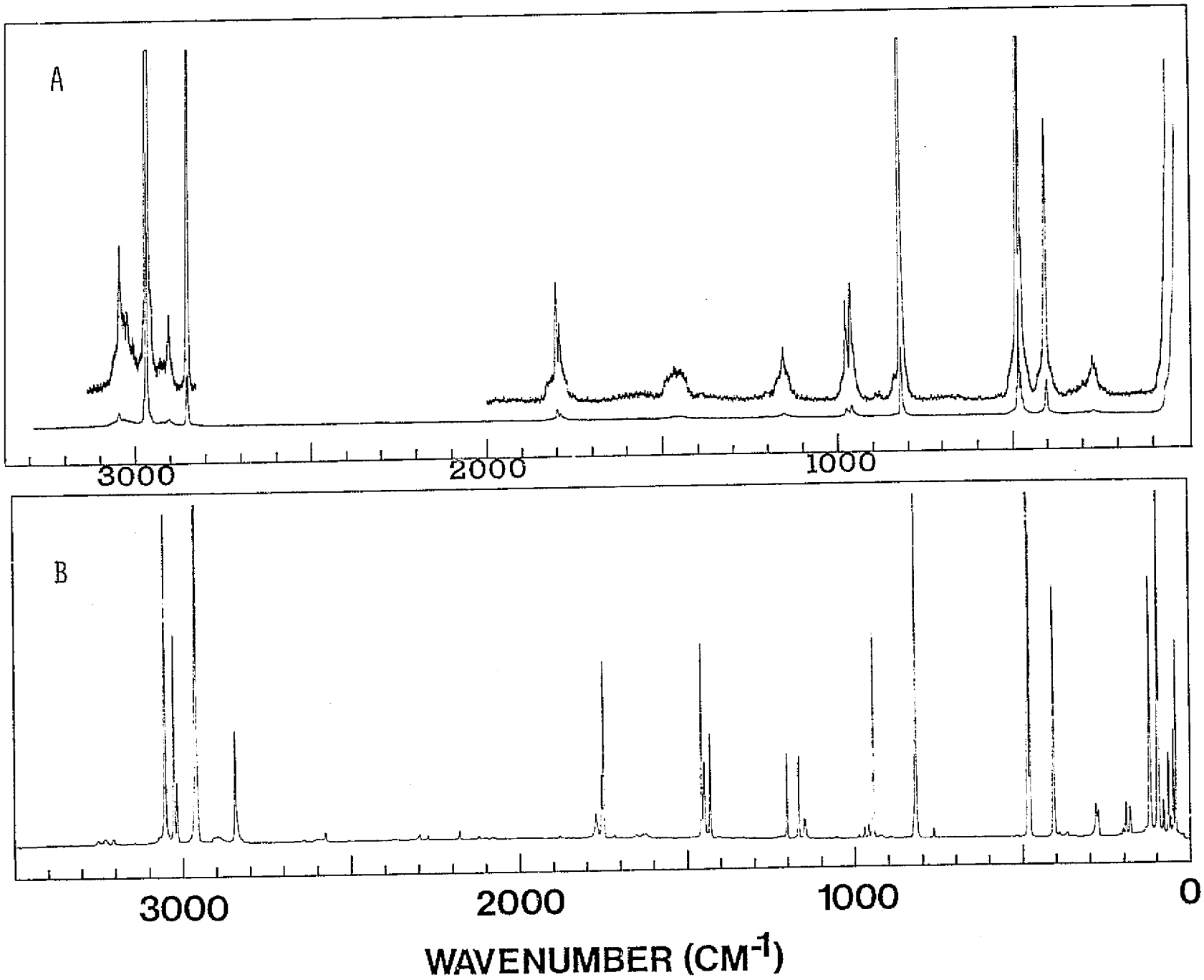
A
3000
2000
1000
B
3000
2000
1000
0
WAVENUMBER (CM-1)

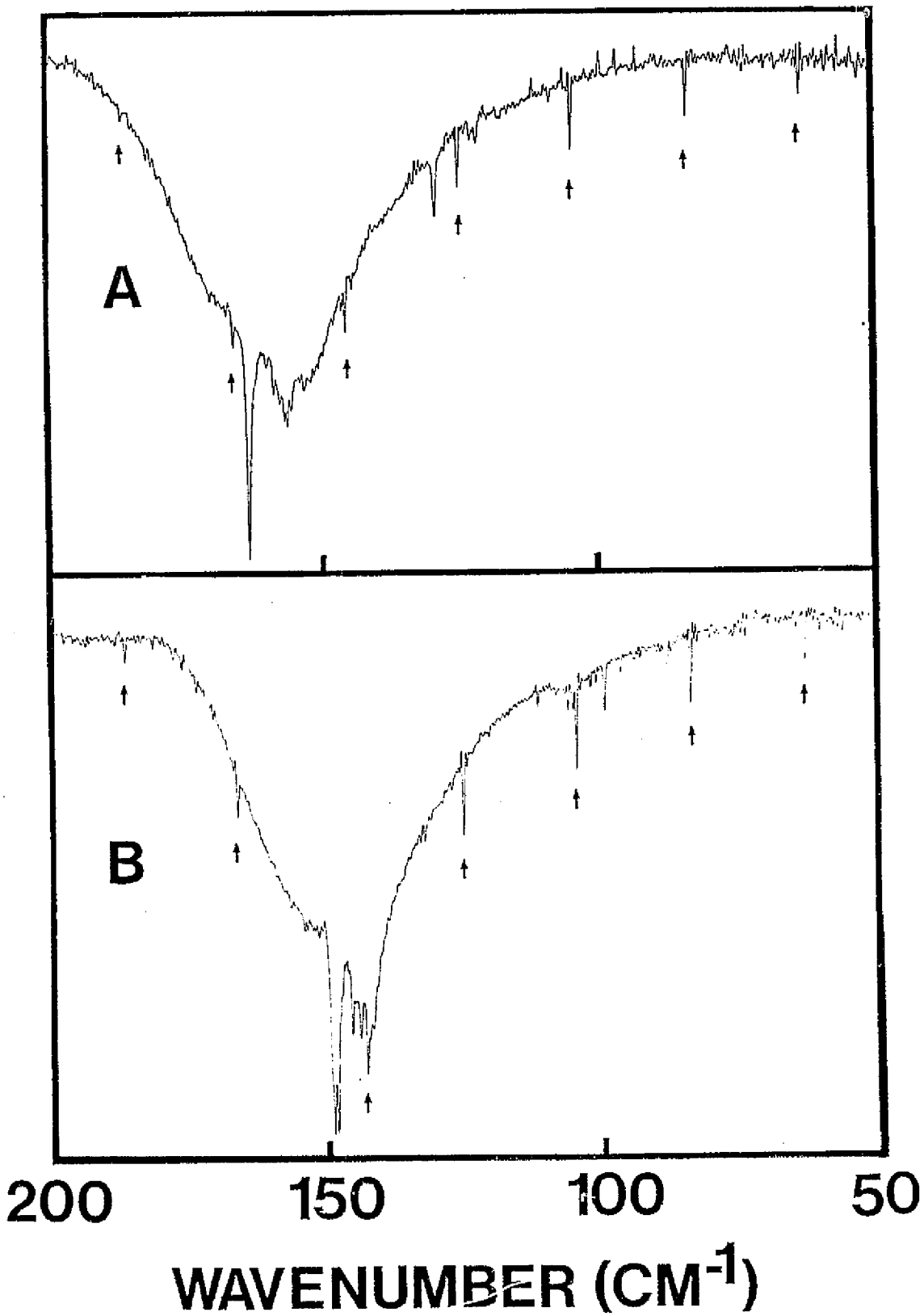
A
B
200
150
100
50
WAVENUMBER (CM-1)

APPENDIX II

SPECTRA AND STRUCTURE OF ORGANOPHOSPHORUS COMPOUNDS. XVII. INFRARED AND RAMAN SPECTRA, VIBRATIONAL ASSIGNMENT AND BARRIERS TO INTERNAL ROTATION FOR t-BUTYLPHOSPHINE

Abstract

The infrared spectra of gaseous and solid tertiary-butylphosphine, $[(CH_3)_3CPH_2]$, have been recorded from 50 cm^{-1} to 3500 cm^{-1}. The Raman spectra of gaseous, liquid and solid $(CH_3)_3CPH_2$ have been recorded from 10 to 3500 cm^{-1}. A vibrational assignment of the 42 normal modes has been made. A harmonic approximation of the methyl torsional barrier from observed transitions in the solid state gave a result of 4.22 kcal/mole and 3.81 kcal/mole in the gaseous state. Hot band transitions for the phosphino torsional mode have been observed. The potential function for internal rotation about the C-P bond has been calculated. The two potential constants were determined to be:

V_3 = 2.79±0.01 kcal/mole and V_6 = 0.07±0.01 kcal/mole.

INTRODUCTION

Vibrational spectrosocopy has been shown to be a valuable tool in the determination of intramolecular potential functions governing internal rotation about single bonds.[1, 2] This method has recently been extended to the study of asymmetric tops rotating against a molecular frame, as opposed to the more familiar symmetric tops such as $-CH_3$ and $-SiH_3$.[3] If the molecular frame is asymmetric as well, it is possible for there to be spectroscopically distinct rotational isomers or conformers. Both ethylphosphine ($CH_3CH_2PH_2$) and isopropylphosphine [$(CH_3)_2CHPH_2$] are examples of this type of system since the PH_2 group constitutes an asymmetric internal rotor. The internal rotation barrier for the PH_2 top has been determined for both of these molecules.[4, 5] If, however, the molecular frame is symmetric, as is the case in tertiary-butylphosphine, [$(CH_3)_3CPH_2$], only one conformation is possible and the potential function governing internal rotation is considerably simplified, becoming three-fold symmetric as in the case of methylphosphine (CH_3PH_2). Thus, the determination of this potential function for t-butylphosphine is a natural extension of the prior studies of ethyl-[4] and isopropylphosphine.[5] Also, it would be of interest to determine the barriers to internal rotation of the methyl groups in this molecule, as part of continuing studies[6, 7] of the top-top interactions in such "three-top" molecules.

Finally, the assignment of the vibrational spectrum of t-butylphosphine would finish the series of singly alkyl-substituted phosphines: methyl, ethyl and isopropyl. Group frequencies determined

for the PH_2 moiety from these studies could be expected to apply to almost any hydrocarbon derivative.

EXPERIMENTAL

In general, all sample preparations and manipulations were performed using standard high vacuum techniques where possible. This was done in view of the relative instability of trivalent phosphorous compounds with respect to oxidation as well as to minimize exposure to the compounds, which are probably quite toxic and undeniably unpleasant smelling. Sample purifications were performed using fractional condensation (trap-to-trap) methods or more generally a low temperature, low pressure fractionating column.

The sample of $(CH_3)_3CPH_2$ was prepared by the reduction of $(CH_3)_2CHPCl_2$ with $LiAlH_4$ in di-n-butyl ether. After low temperature distillation, the purity of the $(CH_3)_3CPH_2$ was checked by mass spectrometry and ^1H, ^{13}C and ^{31}P NMR.

Mid-infrared spectra of $(CH_3)_3CPH_2$ were obtained using a Digilab FTS-15B Fourier transform interferometric spectrometer. A germanium beamsplitter on a KBr substrate gave spectral coverage in the range from 3800 cm^{-1} to 400 cm^{-1}. Spectra of the gaseous phase were obtained by using a 10 cm cell with KBr windows and typically less than 10 torr of sample pressure.

Atmospheric water vapor was removed from the spectrometer housing by purging with dry nitrogen. Since the FTS system uses a He-Ne laser as a frequency reference of relatively high stability, calibration is achieved by adjusting a software parameter, the laser wave length, to reproduce an observed vibrational transition of a suitable standard at its correct frequency. As a result, the accuracy of a measured frequency can be expected to be at least 0.1 cm^{-1} throughout the spectrum.

Both apodization function and resolution were varied for each sample to attain the best quality spectrum, but a typical experiment would be run at an effective resolution of better than 0.5 cm^{-1} using a modified "boxcar" apodization function for photometric accuracy.

Far infrared spectra were obtained by using the FTS-15B and substituting a mylar beamsplitter for the germanium one to obtain a spectral range of 400 to 80 cm^{-1}. A high pressure Hg arc lamp source was substituted for the glower used in the mid-infrared, but otherwise the operation of the instrument was the same as described above. Spectra of compounds in the gas phase were obtained by using 10 cm cells equipped with polyethylene windows. Typical sample pressures ranged from 100 to 300 torr, and spectra were taken at various resolutions between 0.5 and 2.0 cm^{-1}. The spectrum of the solid phase sample was obtained by condensing the sample onto a wedged silicon plate cooled to ∿15°K by a closed cycle He refrigerator.

Raman spectra were recorded to 4000 cm^{-1} using a Cary 82 spectrometer equipped with either a Spectra Physics model 171 or a Coherent Radiation Labs model 53A argon ion laser operating on the 5145 Å line. Spectra of the gaseous phase were obtained using the Cary multipass accessory at sample pressures of ∿300 torr. The spectrum of the liquid was recorded from samples in sealed glass capillaries. The spectrum of the solid was obtained by condensing the sample on a copper block maintained at ∿ -190°C by boiling nitrogen. Polarization measurements were made using the standard Cary accessories. Frequencies measured for sharp, resolvable bands are expected to be accurate to at least ±2 cm^{-1}.

VIBRATIONAL ASSIGNMENT

Tertiary-butylphosphine was assumed to adopt a fully staggered molecular conformation, and as such would possess a single plane of symmetry and belong to the point group C_s. However, if one ignores the hydrogen atoms attached to the phosphorus atom, the molecular symmetry would be C_{3v}. If the major portion of the molecule follows this "local" symmetry, the assignment of the vibrational spectra would be somewhat simplified. Pritchard and Nelson[8] were able to analyze the spectrum of t-butanol using the higher symmetry model for all but a few vibrational modes. Hence for $(CH_3)_3CP$ there would be 24 normal modes, distributed $8A_1$, $4A_2$ and 12E. Under C_s symmetry, $(CH_3)_3CPH_2$ would exhibit 23A' and 19A" vibrational modes. Spectra taken of $(CH_3)_3CPH_2$ in the fluid phases might be expected then to show groups of unresolved bands. However, spectra taken of the sample in the solid phase should allow observation of all 42 fundamentals since in the crystal closely spaced fundamentals should be resolvable. Where applicable, the origin of the vibrational mode under the hypothetical C_{3v} symmetry will be indicated in parenthesis as a guide to the assignment. To aid in the analysis of gas phase band contours, the principal moments of inertia for $(CH_3)_3CPH_2$ were calculated using a reasonable assumed structure. These calculations indicate that the molecule is very nearly a symmetric top, with the A and C inertial axes in the symmetry plane. Thus the A' vibrations are expected to show A/C

hybrid band contours with a sharp Q branch, and A" vibrations B type bands with no central maximum. The vibrational frequencies given in Table I for the A" modes in the infrared spectra of gaseous $(CH_3)_3CPH_2$ therefore reflect estimates of the band center. The vibrational assignments were guided by those of Pritchard and Nelson[8] for $(CH_3)_3COH$ and those of Evans and Lo[9] for $(CH_3)_3CCl$.

The Raman spectra of $(CH_3)_3CPH_2$ in the gaseous, liquid and solid phases are shown in Fig. 1, and the mid-infrared spectra of $(CH_3)_3CPH_2$ in the gaseous and solid phases are shown in Fig. 2. Fig. 3 depicts the far-infrared spectra of gaseous and solid $(CH_3)_3CPH_2$. The observed frequencies and their assignments are given in Table I.

The C-H stretching region, 2870 to 3000 cm^{-1}, showed a dense cluster of bands in all sample phases in both the Raman and infrared spectra. In addition to the 9 fundamentals expected in this region, Durig, et al.,[10] have pointed out that additional strong bands may be expected to occur in this region, attributable to overtones of the antisymmetric methyl deformations in Fermi resonance with the stretching fundamentals. The bands in this region were not resolved even in the spectra of the solid phase, and no additional isotopic species were available for study. In view of these difficulties, attempts to assign this portion of the vibrational spectra were abandoned and the observed band maxima tabulated.

The two very strong bands at 2293 cm^{-1} and 2278 cm^{-1} in the spectra of the solid sample are undoubtedly the antisymmetric and symmetric P-H stretches, ν_{28} and ν_6, respectively. As previous experience has indicated,[4, 5] only the A' mode is seen in the Raman spectra of the gas phase.

The advantage of recording spectra of the solid phase is easily seen in the analysis of the CH_3 antisymmetric deformations ν_{29}, ν_7 (E), ν_{30}, ν_8 (E), ν_9 (A_1) and ν_{31} (A_2). The Raman spectrum of gaseous $(CH_3)_3CPH_2$ shows only a broad, featureless band centered near 1450, but the Raman spectrum of the solid clearly shows all six fundamentals. The assignment of the CH_3 symmetric deformations, ν_{10} (A_1), ν_{11} and ν_{32} (E) is also straightforward, although these modes are not seen in the Raman spectra of the fluid phases.

Assignment of the vibrational spectrum in the region between 1200 cm^{-1} and 800 cm^{-1} is clearly the most difficult. Twelve fundamental vibrations; 6 methyl rocks, 3 C-C stretches and the 3 PH_2 deformations, are all expected to occur in this region. In addition, severe mixing of several vibrational modes, especially the C-C stretches and methyl rocking modes, could make relative intensities unreliable as assignment aids. Three fundamentals of this group should fall considerably lower than the rest; ν_{17} (A_1), the C-C symmetric stretch should be below 900 cm^{-1}, as should ν_{37}, the PH_2 twist, and ν_{18}, the PH_2 wag. Only ν_{17} and ν_{18} should exhibit sharp Q branches in the gaseous phase Raman spectrum, and only three bands are apparent in this region in the Raman spectrum of the solid phase. Thus, ν_{17}, ν_{37} and ν_{18} are assigned to the bands at 836 cm^{-1}, 818 cm^{-1} and 795 cm^{-1} in the Raman spectrum of the solid sample. The frequency of ν_{15}, the PH_2 scissoring mode, is well established [4, 5, 11] and is assigned to the band at 1074 cm^{-1} in the mid-infrared spectrum of solid $(CH_3)_3CPH_2$. The C-C antisymmetric stretches, ν_{33} and ν_{12} (E), occurred near 1240 cm^{-1} in both $(CH_3)CCl$[9] and $(CH_3)COH$;[8] however, there are no bands in this region for $(CH_3)_3CPH_2$.

There are two strong bands at 1211 cm^{-1} and 1192 cm^{-1} in the Raman spectrum of the solid, and have been assigned to ν_{33} and ν_{12}, respectively. The slightly lower, weaker band at 1170 is assigned to ν_{13} (A_1), a CH_3 rocking mode. The complex series of bands seen on the low frequency side of ν_{13} in the gas phase spectra are most probably hot bands due to the methyl torsions or phosphino torsion. Although this assignment of ν_{13} may seem to place this rocking mode quite high, the corresponding modes in $(CH_3)_3COH$ [8] and $(CH_3)_3CCl$ [9] were assigned to bands at 1189 cm^{-1} and 1115 cm^{-1}, respectively. The sharp, polarized peak seen at 1029 cm^{-1} in the Raman spectra of the gaseous and liquid phases must be due to the A' methyl rocking mode, ν_{16}. The sharp, moderately intense Q branch observed at 1090 cm^{-1} in the mid-infrared spectrum of gaseous $(CH_3)_3CPH_2$ must then belong to the remaining A' methyl rocking mode, ν_{14}. In terms of the C_{3v} model symmetry, ν_{14} and ν_{34} are derived from a degenerate E vibration, as are ν_{16} and ν_{35}. Therefore ν_{34} and ν_{35} which would be expected to be clearly discernable only in the solid phase spectra, should fall near their respective A' modes, ν_{14} and ν_{16}. On this basis, ν_{34} is assigned to a band seen at 1065 cm^{-1} in the spectra of the solid phase, and ν_{35} to the band at 1036 cm^{-1}. The remaining rocking mode ν_{36} (A_2) can then be assigned to the broad, depolarized band seen near 940 cm^{-1}.

The assignment of ν_{19}, the C-P stretch, is unambiguous, as it is usually [4, 5] the most intense band in the Raman spectrum below 2000 cm^{-1}. In contrast, this band, located near 590 cm^{-1}, is quite weak in the mid-infrared spectrum.

In the region below 400 cm^{-1} there should be 5 skeletal deformations

as well as the 4 torsional vibrations. In the far infrared spectrum of gaseous $(CH_3)_3CPH_2$ there are apparently two sharp Q branches at 352 cm^{-1} and 346 cm^{-1}, also seen in the Raman spectrum of the gas. However, this structure disappears upon condensation, and only a single, strong, sharp band is seen in the solid phase spectra at 353 cm^{-1}. This band has been assigned to ν_{21} (A_1), the CCC symmetric deformation, with the 346 cm^{-1} band assigned as a hot band. The other two CCC deformations, ν_{38} and ν_{20} (E), are assigned to the bands at 394 cm^{-1} and 389 cm^{-1}, respectively, in the Raman spectrum of the solid. The CCP deformational modes, ν_{39} and ν_{22} (E), have been assigned to the bands at 297 cm^{-1} and 295 cm^{-1}, respectively, in the Raman spectrum of the solid. The anomalously low intensity of ν_{38}, ν_{20}, ν_{39} and ν_{22} in the far infrared spectrum of solid $(CH_3)CPH_2$ is possibly attributable to crystal effects. Following the assignments of Durig, et al.,[7] for a series of t-butyl compounds, the bands at 278 cm^{-1}, 273 cm^{-1}, and 248 cm^{-1} in the far infrared spectrum of the solid have been assigned to the methyl torsional modes, ν_{23}, ν_{40} (E) and ν_{41} (A_2). The strong band system centered near 176 cm^{-1} in the far infrared spectrum of the gas is undoubtedly due to the fundamental PH_2 torsion, ν_{42}, and its hot bands. This band becomes a single sharp band centered at 200 cm^{-1} upon solidification.

DETERMINATION OF THE TORSIONAL BARRIERS

In order to treat the problem of the barriers to internal rotation of the methyl groups in t-butylphosphine, the assumption was made that, so far as the methyl torsions are concerned, the molecule has C_{3v}

symmetry. Lide and Mann[12] have expressed the internal potential energy of such a system in a three dimensional Fourier expansion in terms of $3n\phi_1$, $3n\phi_2$, and $3n\phi_3$, where ϕ_j is the internal rotation angle of the jth top. If terms with n>1 are ignored, the potential energy becomes:

$$2V = V_0 - V_1 \sum_{i=1}^{3} \cos 3\phi_i - V_2 \sum_{i>j} \cos 3\phi_i \cos 3\phi_j - V_3 \cos 3\phi_1 \cos 3\phi_2 \cos +$$

$$V_4 \sum_{i>j} \sin 3\phi_i \sin 3\phi_j + V_5 \sum_{i\neq j\neq k} \cos 3\phi_i \sin 3\phi_j \sin 3\phi_k$$

with the inclusion of the proper kinetic energy terms, the torsional frequencies are given in the harmonic approximation by:[12]

$$\nu_A = [2(F-F')(K + 2L)]^{1/2}$$

$$\nu_E = [2(F + 2F')(K - L)]^{1/2}$$

where

$$K = (9/2)\ (V_1 + 2V_2 + V_3)$$

$$L = (9/2)(V_4 + V_5)$$

The kinetic terms for the present case were obtained by averaging the terms for each top, which were only slightly different. The results of a calculation using this approximation are shown in Table II for both the solid phase and gas phase data. If the interaction constant L is interpreted as a measure of the forces between hydrogen atoms on different CH_3 groups, then the negative sign found for L indicates that the net force is repulsive. Thus, the A_2 - type motion, in which the three tops move in phase, is more effective in keeping the hydrogen atoms apart than the E torsion, where one top is out of phase. In view of the small value found for L, the cosine interaction terms are probably negligible also and (2/9)K is a good approximation of the total barrier.

To determine the barrier to internal rotation of the PH_2 top, a computer program was used which is similar to one described by Lewis, et al.[13] It is assumed that the torsional potential can be represented as a Fourier cosine series in the internal rotation angle:

$$V(\phi) = (\frac{1}{2n}) V_n(1-\cos n\phi).$$

Since the potential function must be three-fold symmetric, only terms where n=3 and 6 were used. The band centers of the $1 \leftarrow 0$ and $2 \leftarrow 0$ phosphino torsions were estimated from the observed far infrared spectrum of the gaseous phase. At this point, the program was allowed to iterate on the two potential constants, and a prediction made for the location of the $3 \leftarrow 2$ transition using the resulting potential function. A slight change in the band contour at 162 cm^{-1} had been noted previously and coincided reasonably well with the prediction. This band was then included in the program input and the potential function re-evaluated. The calculated $4 \leftarrow 3$ transition splits by ≈ 3 cm^{-1} as the energy levels near the top of the well, due to quantum mechanical tunnelling.[14] This predicted transition roughly coincided with another contour change seen at about 151 cm^{-1}; however, this transition was not included in the fit. The results of this calculation are shown in Table III.

DISCUSSION

With regard to the vibrational assignment, several small points are probably ambiguous, but overall it is felt that the given assignment is quite reasonable. A vibrational study of the $(CH_3)_2CPD_2$ isotope would confirm the assignment of PH_2 deformations, and might clarify the

assignment of the skeletal deformations if vibrational coupling of these modes is sufficient to cause an appreciable frequency shift.

The methyl barrier potential constants determined in this work may be compared with those found by Durig, et al.,[7] for some similar molecules observed in the solid state. The (2/9)K term for $(CH_3)_3COH$ of 4.13 kcal/mole goes to 4.41 kcal/mole in $(CH_3)_3CSH$, while the (2/9)L terms are 0.44 and 0.49 kcal/mole, respectively. In comparison, the (2/9)K term for $(CH_3)_3CNH_2$, is 4.28 kcal/mole and 4.22 kcal/mole for $(CH_3)_3CPH_2$, with the (2/9)L terms 0.70 and 0.15 kcal/mole, respectively. The general agreement in the magnitude of (2/9)K is reassuring; however, the trends in the magnitude of (2/9)L for the amine and phosphine are not clearly understood. The magnitude of the (2/9)L term is derived from the frequency splitting of the pseudo-E torsional mode and the pseudo-A_2 torsional mode. Differing degrees of intermolecular effects in the solid, such as hydrogen bonding, might be expected to produce some variation in this interaction term, but the trend should then also be apparent in the $(CH_3)_3COH \rightarrow (CH_3)_3CSH$ series. Similar arguments concerning lone pair effects or lengths of the tertiary carbon to unique substituent bond should be evident in the $(CH_3)_3COH \rightarrow (CH_3)_3CSH$ series, also. The most probable explanation is that the methyl torsional modes in $(CH_3)_3CNH_2$ are severly coupled with the amine torsional vibration which falls between the two methyl torsional regions. Thus the large interaction term seen for $(CH_3)_3CNH_2$ is due in part to interactions of the methyl torsions with the NH_2 torsion.

The barrier to internal rotation of the PH_2 group in $(CH_3)_3CPH_2$, 2.79 kcal/mole, is somewhat higher than that determined by Tsuboi,

et al.,[15] for $(CH_3)_3CNH_2$, 2.36 kcal/mole. The barrier for t-butylphosphine is nearly a kilocalorie/mole higher than the barrier for CH_3PH_2,[11] determined to be 1.96 kcal/mole. Similarly the barrier in CH_3NH_2 is 1.95 kcal/mole.[16] From these results, one might infer that electrostatic interactions of the PH bonds and phosphorus lone pair are greater with CC bonds than with CH bonds, if these interactions are predominantly repulsive.

ACKNOWLEDGEMENT

The authors gratefully acknowledge the financial support given this study by the National Aeronautics and Space Administration through grant NGL-41-002-003. Acknowledgement is also given to the National Science Foundation for funds to purchase the Digilab FTS-15B interferometer by grant MPS-75-06926.

BIBLIOGRAPHY

1. J. R. Durig, S. M. Craven, and W. C. Harris, Vibrational Spectra and Structure, Vol. 1, J. R. Durig, ed., Marcel Dekker, New York, N.Y., (1972) 73-179.

2. A. V. Cunliffe, Internal Rotation in Molecules, W. J. Orville-Thomas, ed., John Wiley and Sons, New York, N.Y., (1974) 217-252.

3. W. G. Fateley, Pure App. Chem., 36, (1973) 119.

4. J. R. Durig and A. W. Cox, Jr., J. Chem. Phys., 63, (1975) 2303.

5. J. R. Durig and A. W. Cox, Jr., J. Phys. Chem., 80, (1976) 000.

6. J. R. Durig, S. M. Craven and J. Bragin, J. Chem. Phys., 51, (1969) 5663.

7. J. R. Durig, S. M. Craven, J. H. Mulligan and C. W. Hawley, J. Chem. Phys., 58, (1973) 1281.

8. J. G. Pritchard and H. M. Nelson, J. Phys. Chem., 64, (1960) 795.

9. J. C. Evans and G. Y.-S. Lo, J. Amer. Chem. Soc., 88, (1966) 2118.

10. J. R. Durig, J. W. Thompson, V. W. Thyagesan and J. D. Witt, J. Mol. Struct., 24, (1975) 41.

11. T. Kojima, E. L. Breig and C. C. Lin, J. Chem. Phys., 35, (1961) 2139.

12. D. R. Lide, Jr., and D. E. Mann, J. Chem. Phys., 28, (1958) 572.

13. J. D. Lewis, T. B. Malloy, Jr., T. H. Chao and J. Leane, J. Mol. Struct., 12, (1972) 427.

14. M. D. Harmony, Chem. Soc. Rev., Vol. 1, The Chemical Society, London, (1972) 211.

15. M. Tsuboi, A. Y. Hirakawa, K. Tamagake, Nippon Kagaku Zasshi, 89 (a), (1968) 821.

16. D. Kivelson and D. R. Lide, Jr., J. Chem. Phys., 27, (1957) 353.

Table I Vibrational Frequencies (cm^{-1}) and their Assignments for t-Butylphosphine.[a]

Infrared gas	Rel. Int.	Infrared solid	Rel. Int.	Raman gas	Rel. Int.	Raman Liquid	Rel. Int.	Raman Solid	Rel. Int.	Assignment
2967	vs									
2960	vs							2959	s,sh	
2954	vs									
		2949	vs	2961	s p	2953	s p	2949	vvs	
2946	vs,sh			2947	s,sh p	2936	s,sh p	2943	s,sh	
		2937	vs							
				2934	vs p	2925	vs p	2930	s,sh	
		2924	s							$\nu_1,\nu_2,\nu_3,\nu_4,\nu_5$ νC-H sym.
								2910	m,sh	$\nu_{24},\nu_{25},\nu_{26},\nu_{27}$ νC-H asym.
		2892	s					2894	vvs	
2906	s			2907	vvs p					
		2877	s					2878	s,sh	
		2857	vs					2861	s	
2873	s			2875	vs p	2865	vs p			
								2850	s,sh	
				2786	m p	2767	m p	2769	m	$2\nu_8$?
				2724	s p	2715	m p	2707	m	$2\nu_{10}$?
		2279	vvs			2284		2293	vvs	ν_{28}
2292	vvs	2293	vvs	2292	vvs p			2278	vvs	ν_6 } νP-H

Table I (continued)

Infrared gas	Rel. Int.	Infrared solid	Rel. Int.	Raman gas	Rel. Int.	Raman Liquid	Rel. Int.	Raman Solid	Rel. Int.	Assignment
								1473	w	ν_{29}
		1467	m,sh							
1476	s,sh							1463	m	ν_7
		1462	vs					1462	m,sh	ν_{30} δCH_3 asym.
				1450	w,brd dp?	1458	w,brd dp?			
1466	s	1457	s,sh					1457	s	ν_8
1456	s,sh	1442	m,sh			1445	w,brd	1442	s	ν_9
		1436	w,sh					1438	m,sh	ν_{31}
1370	s	1368	m,sh							ν_{10}
		1363	s,sh					1363	vw	ν_{11} δCH_3 sym.
1361	s,sh									
		1361	s					1361	vw,sh	ν_{32}
1204	m	1211	w,sh	1205	w,sh			1211	s	ν_{33}
1198	m	1192	m	1199	m p	1192	m,brd p	1192	s	ν_{12} ν_{C-C} asym
1192	m	1169	w	1192	m p	1173	w,sh p	1170	w,sh	ν_{13} ρCH_3
1183	m			1184	w,sh					"hot" bands of ν_{12}
1172	w			1173	w,sh					
1090	m	1096	s			1089	vw,sh p	1092	vw	ν_{14} ρCH_3
1074	m	1074	m	1080	vw,brd p	1072	ww,brd p	1075	m	ν_{15} ρPH_2 sic
		1065	w,sh					1065	w,sh	ν_{34}
		1036	w,sh					1036	w,sh	ν_{35} ρCH_3
				1029	vw p	1029	vw p			
1029	m	1029	m					1032	w	ν_{16}
940	w	938	w	940	vw dp	938	vw,brd dp	937	m	ν_{36}

Table I (continued)

Infrared gas	Rel. Int.	Infrared gas	Rel. Int.	Raman gas	Rel. Int.	Raman Liquid	Rel. Int.	Raman Solid	Rel. Int.	Assignment
834	m	834	w	835	m p	833	w p	836	vs	ν_{17} ν_{C-C} sym.
826	s	816	m	825	w dp	820	vw,sh dp?	818	m	ν_{37} δPH_2 twist
799	s	793	vs	800	s p	798	m p	795	m	ν_{18} δPH_2 wag
589[b]	m	592	w	590	vs p	589	vs p	593	vs	ν_{19} ν_{C-P}
394	w							394	vw,sh	ν_{36} δCCC asym.
		383[b]	vw	382	vw,sh	386	vw,sh			
389	w							389	m	ν_{20} δCCC asym.
352	s	354	s	354	s p	354	m p	353	s	ν_{21} δCCC sym.
346	m			347	w,sh p					"hot" band of ν_{21}
								297	w,sh	ν_{39} δCCP sym.
285	w	295	vw			287	vw,brd dp?			
								295	w	ν_{22} δCCP asym.
		278	s,sh	280	w,brd					ν_{23} τCH_3
266	w					272	vw,sh p?	276	w	
		273	s							ν_{40} τCH_3
227	w	248	w,brd			239	vvw,brd dp	248	vw	ν_{41} τCH_3
181	s	200	vs	172	vvw,brd dp	182	vvw,brd dp	199	vw	ν_{42} τPH_2
171	s									"hot"band of ν_{42}
								77		Lattice modes
								63		
								50		
								42		
								32		

[a]Abbreviations used: s, strong; m, medium; w, weak; v, very; brd, broad; sh, shoulder; p, polarized, dp, depolarized.

[b]This and lower frequencies obtained from the far infrared spectra.

TABLE II METHYL TORSIONAL FREQUENCIES AND POTENTIAL CONSTANTS FOR T-BUTYLPHOSPHINE

	Solid	Gas
ν_E[a] (cm^{-1})	275.5	266
ν_A (cm^{-1})	248	227
F (cm^{-1})	5.3559	5.3559
F' (cm^{-1})	0.0278	0.0278
2/9K(kcal/mole)	4.22	3.81
2/9L(kcal/mole)	-0.15	-0.20

a) $\frac{1}{2}(A' + A'')$

TABLE III PHOSPHINO TORSIONAL FREQUENCIES (cm^{-1}) AND POTENTIAL CONSTANTS

Transition	frequency		
	obs.	calc.	obs.-calc.
1←0	181	180.9	0.1
2←1	172	172.2	-0.2
3←2	162	161.8	0.2
$4\leftarrow3^-$		146.1	4.9
$4\leftarrow3^+$	$(151)^2$	149.1	0.9
V_3	976 ± 4^b cm^{-1} or 2.79 ± 0.01 kcal/mole		
V_6	-25 ± 2 cm^{-1} or 0.07 ± 0.01 kcal/mole		

a) estimated
b) quoted error limits represent one standard deviation

FIGURE CAPTIONS

Figure 1 Raman spectra of t-butylphosphine

A) gaseous

B) liquid

C) solid

Figure 2 Mid-infrared spectra of t-butylphosphine

A) gaseous, approximately 2 torr sample pressure

B) gaseous, approximately 40 torr sample pressure

C) solid

D) solid, more sample deposited

Figure 3 Far infrared spectra of t-butylphosphine

A) gaseous, approximately 400 torr

B) solid[a]

a) pronounced baseline "roll" is due to interference fringes from the sample film

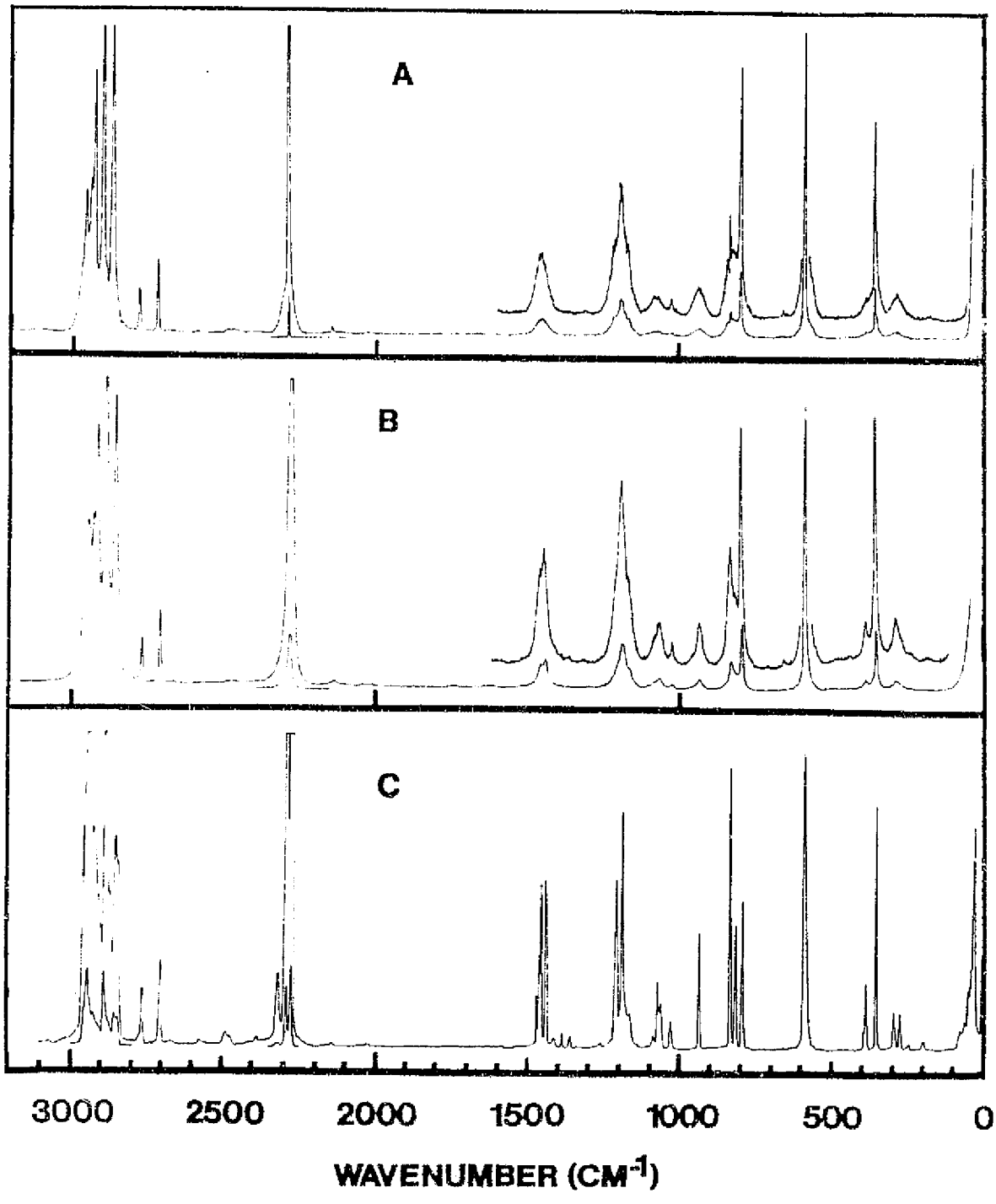
A
B
C
3000
2500
2000
1500
1000
500
0
WAVENUMBER (CM-1)

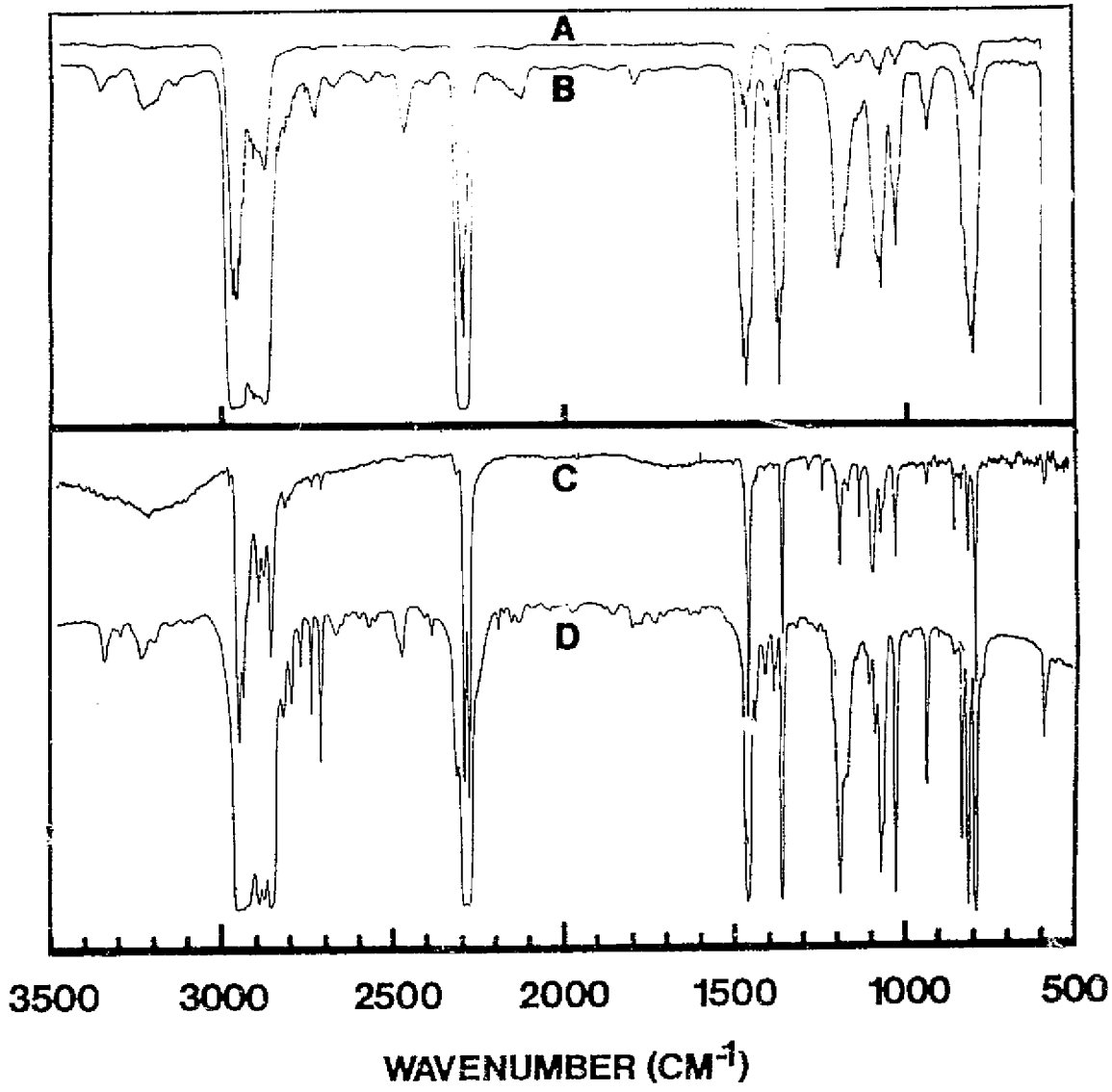
A
B
C
D
3500
3000
2500
2000
1500
1000
500
WAVENUMBER (CM-1)

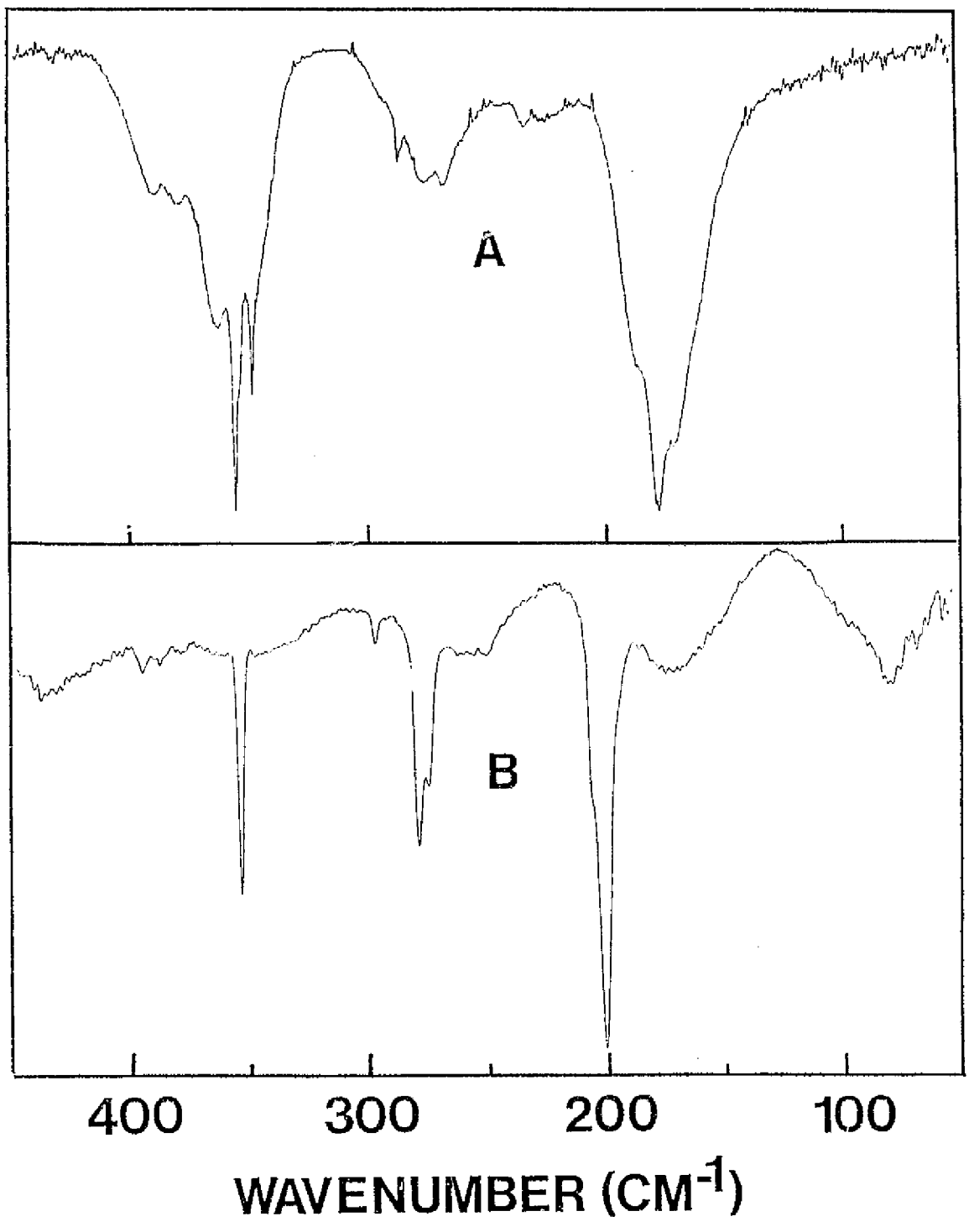
A
B
400
300
200
100
WAVENUMBER (CM-1)